2017

Flinders
UNIVERSITY

Surface Modification of Chalcopyrite and Pyrite by Acidithiobacillus Ferrooxidans

THESIS SUBMITTED FOR PARTIAL FULFILMENT OF THE DEGREE OF MASTER OF SCIENCE IN CHEMISTRY

By Zhen He

Supervisor: Associate Professor Sarah Harmer

Declaration

I certify that this thesis does not incorporate, without acknowledgment, any material previously submitted for a degree or diploma in any university; and that to the best of my knowledge and belief it does not contain any material previous published or written by another person except where due reference is made in the text.

X _____

Zhen He Date: 08/11/2017

Acknowledgement

First of all, I would like to sincerely thank my supervisor Associate Professor Sarah Harmer who gave me this opportunity to do this wonderful project. I have no background knowledge before I choose this project and you provided me endless patience, professional support and encouragement throughout this year and take me step by step to finish this project. Thanks a lot to the Harmer research group for their friendship and the patience they put up with my research project.

Many thanks to the help from Belinda Bleeze, this project would not be possible to successfully complete without her.

I am grateful to the technical support I received from Adelaide Microscopy and their staff Lyn Waterhouse and Ruth William. I am deeply appreciated the SEM support of Dr. Jason Gascooke from Australian Microscopy & Microanalysis Research Facility. Christopher Bassell from the Mawson Lake Campus at University of South Australia, your help on my XPS analysis was gratefully appreciated. Dr. Jing Zhao from Flinders University, your professional assistance on my XRD analysis was greatly appreciated.

Finally, I would like to thanks to my beloved parents and girlfriend for their unconditional love and support.

Table of Contents

List of Figures

List of Tables

Abstract

The negative environmental impacts of the mining industry are well-known and include soil erosion, water pollution and loss of biodiversity (Australian Bureau of Statistics, 2003). One of the main causes of the pollution is the usage of chemical reagents during the mineral separation processes (Besser, 2009). Sulfide minerals are primary separated using froth-flotation. Chalcopyrite is one of the most abundant sources of copper in the world and pyrite is the worthless product produced from the separation of chalcopyrite. Froth-flotation is the most common method used to separate chalcopyrite and gangue minerals. A large amount of environmentally-harmful chemical reagents are used in this mineral separation processes to enhance its efficiencies, such as xanthate and cyanide. Bio-flotation is a new technique which uses microbes to replace those chemical reagents making for a more environmentally-friendly process.

Acidithiobacillus ferrooxidans is one of the most well-studied micro-organisms used in bio-flotation. Bacterial counting, Scanning Electron Microscopy, Elemental Dispersive Analysis by X-ray and X-ray photoelectron spectroscopy were used to determine the selective attachment of *A.f.* on chalcopyrite and pyrite and how it modifies the mineral surface. Micro-froth flotation tests and XRD analyses were performed to investigate how *A.f.* can be used to increase the separation efficiency of chalcopyrite.

The depression of the separation efficiency of pyrite has been observed after expose to *A.f.* for 72 hours which has correlates with the formation of biofilm through its SEM images.

1.0 Introduction

1.1.1 Chalcopyrite and Pyrite

Chalcopyrite is one of the most important sulphide minerals as it is the most abundant source of copper available in the earth's crust. It has a chemical formula of $CuFeS_2$ and the oxidation state of Fe in chalcopyrite is +3, as determined by Mössbauer spectroscopy (Mussel et al., 2007). Each sulphur atom in the crystal structure of chalcopyrite is tetrahedrally surrounded by two copper and two iron atoms, and each metal ion is attached to four sulphur atoms (Vaughan and Craig, 1978).

Pyrite is the most common gangue mineral associated with chalcopyrite. The chemical formula of pyrite is FeS_2 with an oxidation state of Fe (II). The unit cell of pyrite is very similar to sodium chloride. It contains di-sulfide bonds in an octahedral coordination resulting in high crystallographic symmetry (Vaughan and Craig, 1978).

1.1.2 Froth-flotation

In the current mining industry, forth-flotation is used to separate chalcopyrite from the gangue minerals. Its theory is based on the difference in surface properties of chalcopyrite and gangue minerals but still not fully understood due to large variability in ores. As Figure 3 illustrates, the industrial grade compressed air is pumped into the pulp from the top and produces air bubbles with different size and shape. At this point, the addition of frother is able to control the bubble size and shape. The agitator at the bottom of the tank will keep stirring and provide turbulence to stimulate the collision between the mineral particles and air bubbles. Only the highly hydrophobic mineral particles can strongly attach to the air bubbles and lift it to the water surface. This mechanism is the reason why froth-flotation is very selective and can be used to separate specific minerals. This can be achieved by changing the hydrophobicity of the specific mineral surface (Wills, 2011).

The mineral particle size is a critical physical factor in the froth-flotation process as it has to be relatively fine to keep the adhesion force between the minerals and air bubbles strong enough. If the mineral particles are too large, the adhesion between particles and air bubbles will be less than the weight of particles and hence drop the particles (Finch and Dobby 1990). The air bubble size and flow rate are two other physical factor that will affect the recovery efficiency of froth-flotation. In this project, the surface chemistry changes were the focus of this study. Therefore, the mineral particle size, air bubbles and flow rate were kept constant.

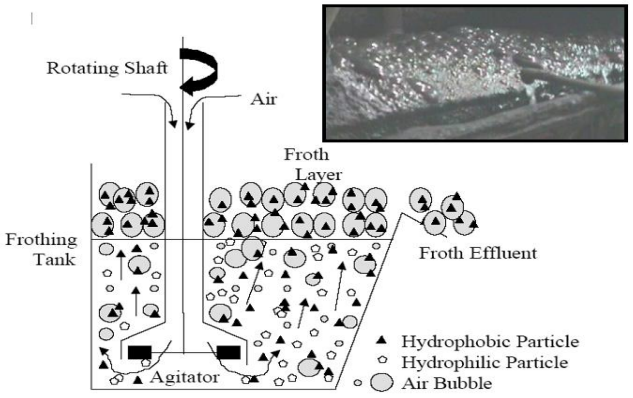

Figure 1: The mechanism of froth-flotation

There are two different mechanisms for separation of the valuable minerals and gangue minerals: direct flotation and reverse flotation. In the direct flotation, the hydrophobicity of valuable mineral particles is increased so they can attach to air bubbles and transfer to the froth, or float fraction; thus the gangue minerals will be left in the pulp or tailing. In the reverse flotation, the gangue minerals are transferred to the froth, leaving the valuable minerals in the tailing (Will, 2011). In this project, the direct flotation was conducted due to the bacteria used being able to depress the recovery of pyrite.

1.1.3 Flotation reagent

Not all of sulfide minerals are naturally hydrophobic. Some chemicals known as flotation reagents are commonly added during the froth-flotation process to enhance the recovery efficiency, such as collectors, depressants and frothers. Frothers can improve the stability of the froth formed by air bubbles and mineral particles. Activators are used to help the collector to adsorb onto the mineral surfaces. Depressant have the opposite effect as a collector which is used to prevent the flotation of gangue minerals by increase their hydrophilicity, e.g. cyanide used in the mining industry. Collectors generally contains a polar head and a non-polar tail. Xanthate is one of the collectors commonly used in froth-flotation of copper ores. It contains a polar di-thiocarbonate group and a non-polar organic group. The polar group can attach to the mineral surface and increases the hydrophobicity by its non-polar group (Will,

2011). However, xanthate is very toxic to aquatic life when the concentration is above 1mg/mL, and the water resources near the mining industry are generally contaminated by this flotation reagent (Xu, 1988).

1.2.1 Acidthiobacillus Ferrooxidans (A.f.)

The bacteria *A.f.* was the first discovered and is the most studied microorganism that is capable of oxidizing metal sulfide. It is a gram-negative rod-shape bacterium and optimally live in the environment with pH 2.5 and 30-35°C. *A.f.* can attach to the metal sulfide and secrete EPS to enhance attachment then form biofilm, as illustrated in Figure 2. This bacterium utilizes the energy from the oxidation of Fe (II) ions and various sulfur compound (such as elemental sulfur and thiosulfate) to support its growth, and form Fe (III) and sulfate ions (Schippers et al., 1996). Hazeu and his co-workers (1988) have discovered the accumulation of fine sulfur deposits when *A.f.* grow on sulfur compounds. Misra and Chen (1995) have reported that *A.f.* will significantly depress the recovery efficiency of pyrite in the flotation of pyrite and galena with xanthate used as a collector. Moreover, it has been reported that pyrite will be dramatically depressed by *A.f.* bacteria in the bio-flotation of low grade Sarcheshmeh copper ore, but chalcopyrite and other sulphide minerals are unaffected (Kolahdoozan *et al.*, 2004; Hosseini *et al.,* 2005).

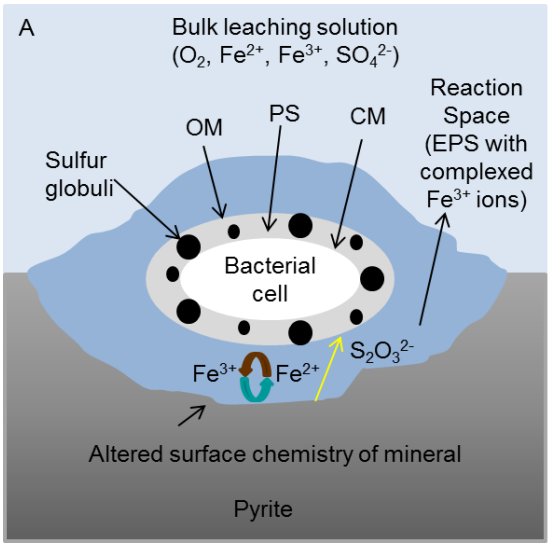

Figure 2： *A.f.* attach to the pyrite surface. CM: Cytoplasmic membrane, PS: periplasmic space, OM: outer Membrane.

Image resource: Associate Professor Sarah Harmer

1.2.2 The role of *A.f.* in oxidation of chalcopyrite and pyrite

Metal sulfides are classified into two groups based on their solubility in acid. Acid-insoluble metal sulfide like pyrite will go through the thiosulfate mechanism. Under acidic conditions, the electron extraction of Fe (II) ions is the only pathway for pyrite to be dissolved resulting in the formation of iron (II) ions and thiosulfate ions in the solution. Further oxidation of those two ions by *A.f.* will form polysulfide. Finally, sulfate ions and more protons are expected to form by oxidation of *A.f.* (Schipppers et al. 1999). The presence of iron (II)-oxidizing bacteria such as *A.f.* and *Leptospirollum ferrooxidans* and Fe (III) ions are able to

leach acid-insoluble metal sulfides at significant rates under acidic conditions (Schipppers et al. 1999). Rohwerder et al. (1998) and Schippers et al. (1999) have reported that the leaching rate of pyrite will be dramatically reduced under acidic conditions without iron (II)-oxidizing bacteria and iron (III) ions.

The key difference between thiosulfate and polysulfide mechanisms is the attacking of protons producing different sulfur compounds during the oxidation of *A.f.* The acid-soluble metal sulfides like chalcopyrite are able to be dissolved by both actions of electron extraction of iron (III) ions and proton attack. Afterwards, sulfide cation (H_2S^+) and iron (II) ions will be formed and spontaneously dimerize to di-sulfide (H_2S_2). Elemental sulfur will be formed by the further oxidation of polysulfide by *A.f.* Finally, sulfate ions and protons will be formed at the end of the oxidation. The proton is recycled to dissolve chalcopyrite (Schipppers et al. 1999). Thus, the solution of *A.f.* grown on chalcopyrite will have higher pH than pyrite as the exposure time increases.

1.2.3 Bio-flotation

Bio-flotation is a biotechnology that uses bacteria to change the surface properties of minerals and enhance the separation efficiency and hence make the mineral processing environmentally-friendly (Pecina-Treviño et al., 2012). Those microorganisms that can be used to replace the flotation reagents are generally naturally found from the deep caves and mining sites. The surface properties of minerals can be altered when bacteria attaching to the surface and oxidize or reduce metal atoms on the surface (Peterson, 2006). Some studies also indicate the extracellular polymeric substances (EPS) produced by bacteria are also able to change the surface properties of minerals. Polysaccharides and lipids are the main components of EPS. It has been reported that the surface of pyrite will be more hydrophilic after the EPS are adsorbed on the surface (Bagdigian & Myerson, 1986).

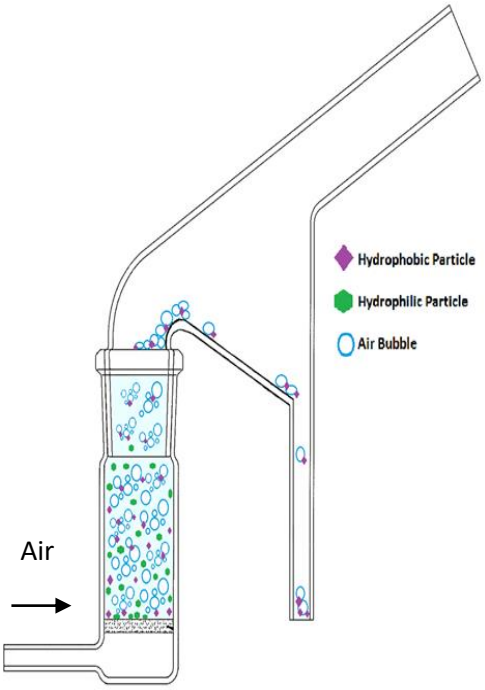

Figure 3: Modified Hallimond tube used in bio-flotation. Image: Belinda Bleeze, personal communication.

2.0 Experimental and Techniques

2.1 Mineral samples

All of the minerals used for experiments in this project have particles with a size of 38-75 µm. Chalcopyrite and pyrite were obtained from China and Peru, respectively. Each mineral was analyzed using total acid digestion method at Flinders Analytical. The concentration of sulfur in both chalcopyrite and pyrite was measured by inductively coupled plasma optical emission spectrometry and other elements were analyzed by inductively coupled plasma mass spectrometry (ICPMS). The concentration of each element in the original chalcopyrite and pyrite is listed in Table 2.1. It indicates that the impurity concentration in pyrite is less than 4%. However, the concentration of impurities in chalcopyrite is almost 16%. All the minerals used in this project were sterilized by ultra-violet light for 15mins twice.

Table 1: The concentration of elements in pyrite and chalcopyrite (%)

MINERAL	Na	Mg	Al	P	Ca	Fe	Cu	S
PYRITE	-	0.005	0.017	-	0.025	45.35	0.068	51.52
CHALCOPYRITE	0.035	0.572	0.088	1.32	2.89	25.55	28.93	29.7

2.2 HH Media Solution

HH media solution was used in this project to culture *A.f.* It consists of solutions A and B. Solution A is made by dissolving 132mg $(NH_4)_2SO_4$, 53mg $MgCl_2{\cdot}6H_2O$, 27mg KH_2PO_4 and 147mg $CaCl{\cdot}2H_2O$ in 950ml Milli-Q water. The pH was then adjusted to 1.8 by adding sulfuric acid. Solution B was made by dissolving 20g of $FeSO_4{\cdot}7H_2O$ in 50 ml by 0.125mol/L sulfuric acid. All of the HH media solutions were sterilized separately by heating at 121°C in autoclaves prior to experiments.

2.3.1 *Acidithiobacillus Ferrooxidans* Cultures

A.f. were cultured in HH media solution A and B and used as reference culture. Solution B contains Fe^{2+} ions and *A.f.* can use it as an energy resource and generate Fe^{3+} ions. The mineral-based cultures used 20g of chalcopyrite or pyrite instead of solution B. All of the cultures were done with 10% inoculation and incubated at 30°C and 155rpm in a Retak Orbital Mixer. The reference culture and *A.f.* grown on pyrite were continuing re-cultured for four years. But *A.f.* grown on chalcopyrite was started from the beginning project.

2.3.2 Growth Cycle

The growth rate of bacteria of the culture is used to classify six different phases in the order of lag phase, acceleration phase, exponential phase, retardation phase, stationary phase and phase of decline. At the beginning of the inoculation, the growth rate of bacteria is equivalent to zero and enters its lag phase. The bacterial growth rate will increase its acceleration phase, and the cell concentration will also increase. When the bacterial growth rate increases steadily, the bacterial growth enters its exponential phase. Once the bacterial growth rate starts to decrease, the retardation phase begins. Next phase is called stationary phase; the bacteria growth rate is equivalent to the bacteria death rate at this stage. The cell concentration during this phase is constant. During the phase of decline, the cell death rate is greater than the cell growth rate and the cell concentration starts to decrease (Fankhauser, 2004).

The re-culture of the reference culture and mineral-based culture were all due on the stationary phase. The *A.f.* reference culture was re-cultured every 96 hours and the *A.f.* pyrite-based culture was re-cultured every 4 weeks. In order to adapt *A.f.* on chalcopyrite, *A.f.* grown on pyrite was taken to expose to mixed minerals (consist of pyrite and chalcopyrite). All the glassware and pipette tips used during the re-culture of reference culture and mineral based culture were sterilized by autoclaved at 121°C.

2.3.3 Bacterial Growth Curve

The growth of the *A.f.* cultures were monitored by bacterial cell counting method. A 10µL aliquot sample was taken from the *A.f.* cultures using an automated pipette and then transferred to a Hemocytometer. An Olympus BX50 phase contrast microscope was used to count the number of bacterial cells in 5 squares of Hemocytometer triplicates at 40× magnification. To make homogenous sample, all cultures were gently agitated before sample collection. The cell concentration of the bacterial cell culture is calculated by the following equation (Freund 1964).

Equation 1:

$$Concentration\ of\ cells\ in\ original\ mixture = \left(\frac{\boldsymbol{number\ of\ cells\ counted}}{(\boldsymbol{proportion\ of\ chamber\ counted})(\boldsymbol{v}_{\ squares\ counted})}\right)\left(\frac{\boldsymbol{volume\ of\ diluted\ sample}}{\boldsymbol{v}_{original\ mixture}}\right)$$

2.4 Ferrous Ion Titration

A.f. can oxidize ferrous (Fe^{2+}) ions to ferric (Fe^{3+}) ions and use the energy to support its growth. Therefore, the ferrous ions concentration in solution is related to the bacterial cell growth. To determine the ferrous ions concentration in the solution, an oxidation-reduction titration was performed using 0.025 mol/L cerium sulfate solution. Equation 2 is the net ionic equation of the titration and used to calculate the ferrous ions concentration (Dhau 2014).

Equation 2: $$Ce^{4+}(aq) + Fe^{2+}(aq) \rightarrow Ce^{3+}(aq) + Fe^{3+}(aq)$$

The volume of cerium sulfate solution used during the titration was taken as the titre value. The number of moles of cerium sulfate used is calculated which is equivalent to the number of moles of ferrous ions in the solution. 10mL sample was taken at each point from the reference culture and then filtered by 0.22µm sterilized single use membrane filter. Each titration was performed using 3mL of filtered sample with one drop of ferrin indicator. The cerium sulfate solution was added drop-wise into the sample solution until the colour of the solution changed. To increase the accuracy and precision of the titration results, titration was conducted in triplicate at each time point.

2.5 Scanning Electron Microscopy (SEM)

2.5.1 Principle of SEM

A focused beam of electrons is used in SEM to scan the sample surface and produce secondary electrons, back-scattered electrons and characteristic X-ray. The high resolution morphological information of the sample surface can be obtained using the secondary electron mode. In this mode, a low energy (approx. 2-50eV) secondary electrons will be emitted from the surface after the electron beam interacts with the surface layers of the sample (McMullan, 2006).

2.5.2 Energy Dispersive X-ray Spectroscopy (EDAX)

In EDAX mode of SEM, a bremsstrahlung x-rays resource will be used to excite and ionize the inner electrons of the atoms on the sample surface. After the inner electrons are excited and ionized, the gap will be filled by outer electrons and releasing the excess energy which emitting characteristic x-ray. These characteristic x-rays can be used to characterize the chemical composition of the sample surface (Goldstein, 2003). In this project, this technique

was used to obtain the semi-quantitative chemical composition of the sample and determine the EPS and bacteria.

2.5.3 SEM Sample Preparation

All mineral samples used to prepare the SEM samples were 38-75µm chalcopyrite and pyrite. Four SEM samples collected at different times were prepared and analyzed in this project to determine the time range of *A.f.* selective attachment on the surface of chalcopyrite and pyrite. These SEM samples including fresh pyrite, fresh chalcopyrite, pyrite exposed to *A.f.* and mixed pyrite and chalcopyrite exposed to *A.f*. The blank samples only contained 20g of minerals and expose to HH media solution A at pH 1.8. All SEM samples were cultured at 30°C and 155 rpm in a Retak Orbital Mixer.

In the single mineral SEM samples 20g of chalcopyrite or pyrite were used and the mixed mineral sample contains 5g pyrite and 5g chalcopyrite. All the minerals were sterilized by ultra-violet light for 15 minutes twice. The blank mineral SEM samples were prepared by 20g of mineral with 200ml sterilized HH media solution A at pH 1.8. The initial bacterial cell concentration of *A.f.* exposed to pyrite or mixed minerals is 1×10^7 cells/ml and *A.f.* were taken from the *A.f.* grown on pyrite culture. All of the samples were taken at 2 hours, 24 hours, 48 hours, 72 hours, 1 week and 2 weeks' exposure time. Once those samples transferred from the *A.f.* culture to 5ml cryogenic tube, those samples were preserved in 1ml of 3% glutaraldehyde electron microscopy (EM) fixative solution which made by 0.84ml phosphate buffered saline (PBS) and 0.16ml glutaraldehyde and store in the fridge at 4°C. The SEM sample preparation was completed at Adelaide Microscopy.

At Adelaide Microscopy, the fixative solution was pipette out and minimum washing buffer (4% sucrose in PBS) was used to cover the mineral samples and exposed for 5 minutes. After taken out the washing buffer, 2% OsO_4 in water were used as second fixative solution to cover the mineral samples and exposed for 30 minutes. After the removal of 2% OsO_4 solution, the mineral samples were dehydrated by exposed to 70% ethanol for 10 minutes twice, 90% ethanol for 10 minutes once and 100% ethanol for 10 minutes three times respectively. The mineral samples were then dehydrated by exposed to 1:1 hexamethyldisilazane (HMDS) and 100% ethanol for 10 minutes and followed by exposure to 100% HMDS for 10 minutes twice. The 100% HMDS were then removed and allow the mineral samples to air dry. After the mineral samples were completely dried, they were

attached to the SEM sample holders and Araldite was used as adhesive. The mineral samples were then dried by nitrogen gas before analysis.

2.5.4 Imaging and EDAX via SEM

All of SEM images and EDAX results were obtained using an Inspect FEI F50 scanning electron microscopy with a field emission gun. Images were obtained at an accelerating voltage of 5kV and a spot size of 3 with a working distance of about 10mm. The secondary electron mode of the SEM was used in this study to determine the bacterial attachment onto the mineral surface and how it change over exposure times.

Energy Dispersive Analysis by X-ray (EDAX) was also used in this project to determine the chemical composition of the components attached to the mineral surface. The analysis was done by first viewing the interested sample surface in SE mode and selecting the interested point. The EDAX spectrum was obtained at 20KV with a spot size of 4.

2.6 X-ray Photoelectron Spectroscopy (XPS)

2.6.1 Principle of XPS

The XPS is an ultra-high vacuum technique that uses a monochromatic x-ray source to irradiate the sample surface and interact with the atoms on the surface then eject the electron. The electron from higher energy orbital will fill the core hole. The energy difference will be measured as binding energy.

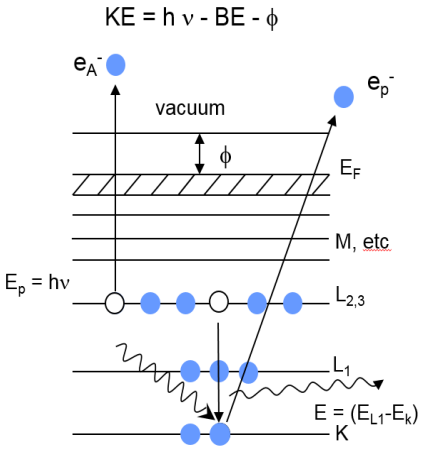

Figure 4: Illustration of photoelectron effects

Ultra-high vacuum system is usually applied to XPS for a better photoelectron collection. Any gases in the chamber will be interact with the electrons which may cause no sufficient energy are collected by analyser (Moulder et al. 1995; Harmer et al. 2006). The binding energy of the emitted electrons is calculated by equation 3 as following. The kinetic energy of the emitted electrons is calculated by the following equation shown in Figure 4. KE represents the kinetic energy of emitted electrons. The photon energy is given by hv where h is the plank's constant and v is the frequency of the photon. BE represents the binding energy of an electron. Φ is the work function which represents the minimum energy required to eject an electron from the solid surface.

Equation 3: $KE = h\nu - BE - \phi_s$

2.6.2 XPS Sample Preparation

All pyrite mineral particles were sterilized by ultra-violet light for 15 minutes twice before used in XPS analysis. Blank pyrite solution was prepared by expose 20g pyrite to 200ml HH media solution A at pH 1.8. Pyrite expose to *A.f.* samples were prepared by expose 20g pyrite to bacteria with a concentration of 1.5×10^7 cells/ml and make up to total 200ml with HH media solution A. Un-reacted pyrite sample was stored in freezer at -80°C before analyzed. The sample was taken at 24 hours, 48 hours, 72 hours and 1 week and transferred to 10ml plastic centrifuge tube, followed by blew nitrogen gas and snap frozen and store in freezer at -80°C until the sample analyzed in the University of South Australia Mawson Lakes Campus.

The XPS samples were defrosted slowly at room temperature before analysis. One drop of de-frosted sample was transferred onto the carbon tape. The solution residue in the mineral samples was removed by using Kimwipe. A spatula was used to spread the mineral sample evenly. The introduction chamber, transfer chamber and analysis chamber were pre-cooled to -168°C prior to introduce the sample. The pressure of all three chambers was set up to 1×10^{-8} Torr or lower. The survey scan spectra, oxygen 1s spectra, sulfur 2p spectra, carbon 1s spectra and Fe 2p spectra were obtained to characterize the chemical composition of the sample surface. As the elemental sulfur will be volatile at temperature above -133°C, a sulfur 2p spectra at ambient temperature (about 20°C) was also obtained to determine the presence of elemental sulfur on the sample surface.

2.6.3 Experiment Setting

The XPS analysis of pyrite samples were conducted by Kratos Axis Ultra XPS in UniSA and a monochromatic soft Al x-ray was used with a photon energy of 1487eV. The step of energy for all spectra collection is 0.1 eV except Fe 2p (0.05 eV).

2.6.4 XPS Data Analysis

CasaXPS software (Fairly, 2009) was used to process and analyze the obtained XPS data. All spectra were calibrated by shifting C 1s peak to 284.8eV (Metson, 1999) and S $2p_{3/2}$ peak to 162.4eV for bulk pyrite. The sensitivity factors in CasaXPS was used to determine the atomic concentrations of major elements (Fairley, 2009). Generally, there are two peaks will be shown as doublets on S 2p spectra which are S $2p_{3/2}$ and S $2p_{1/2}$ due to the spin orbit

splitting. The intensity of the S $2p_{3/2}$ peak is twice that of the S $2p_{1/2}$ peak. The binding energy of the S $2p_{3/2}$ peak is 1.19eV higher than the S $2p_{1/2}$ peak. The background of all spectra was fitted using a Shirley background (Shirley, 1972). A Gaussian-Lorentzian (G/L) function with 50% Gaussian and 50% Lorentzian was used to fit all spectra. Some previous studies were used as reference to fit the S 2p spectra (Harmer et al., 2006; Acres et al., 2010).

2.7 Bio-flotation

2.7.1 Principle of Bio-flotation

The separation efficiency of bio-flotation depends on three physical factors including the particle size, bubble size and flow cell dimensions. The hydrophobicity of the mineral surface is one the chemical factors have impact on the separation efficiency. In this project, the surface modifications of chalcopyrite and pyrite by *A.f.* is the study objective. Therefore, all three physical factors were fixed. The mineral particle size used in flotation test was 38-75µm and the flow rate was set on 0.4L/min. The bubble size depends on the flow rate. Thus, the bubble size will be constant in this study (Bleeze, 2014).

2.7.2 Flotation Test

1g of 38-75µm chalcopyrite or pyrite was used in the single mineral flotation tests. The mixed mineral flotation test was used 1g of mixed mineral consist of 0.5g pyrite and 0.5g chalcopyrite. The baseline flotation tests were conducted using Milli-Q water with NaOH at pH 9 and HH media solution at pH 1.8. The mineral samples were not pre-conditioning in the baseline flotation experiment.

During the pre-conditioning process, the mineral samples were exposed to 20ml of different pre-conditioned solution at 30°C and 155 rpm in a Ratek Orbital Mixer. Potassium Isopropyl Xanthate was used as collector in the flotation test at 1×10^{-4} mol/L. All flotation tests were conducted in duplicate. Table 2.2 is summarized all of the flotation test carried out in this project.

The mineral samples were transferred into the modified Hallimond tube (from Brandon Scientific Glassblowing) after conditioning and 30ml conditioning solution was used to rinse the conditioning flask. The industrial grade compressed air was applied to Hallimond tube to float the mineral samples at a flow rate of 0.4L/min for 5 minutes and stirred by magnetic stirrer. A scintillation vial was used to collect the floated fractions from the collection tube.

The floated fractions were then filtered under vacuum with pre-weighed 5µm Millipore mixed cellulose membrane filter. The gangue fractions were collected with same vacuum filtration process. After the floated fractions and gangue fractions were air dried, both fractions were then weighed.

Table 2: The Summary of Flotation Tests Carried out with Different Exposure Time.

Pre-conditioning Conditions	Exposure Times (Hours)	
	Collectorless	With collector (PIPX)
Milli-Q Water at pH 9 (NaOH)	0, 24,48,72	24,48,72
HH Media at pH 1.8 (Sulfuric acid)	0, 24,48,72	24,48,72
A.f. grown on HH media	24,48,72	24,48,72
A.f. grown on pyrite	24,48,72	24,48,72
A.f. grown on mixed	24,48,72	-

All bacterial conditioning was performed at cell concentration of 1.5×10^7 cells/ml. All glassware used in flotation test were sterilized before use. The floated fractions will be analyzed by quantitative X-ray diffraction. The single mineral recovery efficiency was calculated by equation 4.

$$\text{Equation 4: Recovery (\%)} = \frac{\text{Flotated fraction}}{\text{Flotated fraction+Gangue fraction}} \times 100$$

2.7.3 X-ray Diffraction (XRD)

2.7.3.1 Principle of XRD

XRD is a technique used for determining the crystal structure of a compound and it also can be used to distinguish two different polymorphic substances. A monochromatic x-ray resource is generated by cathode ray tube and filtration and then it directly towards the sample surface and interact with the surface crystal structure of the sample. The diffracted x-rays are detected and interpreted by Bragg's law as equation 5 shown. It can be used to analyze the angular difference between the x-rays and the diffracted fluorescent photon (Jenkins and Snyder, 2012). The crystal structure of the sample can be determined by Bragg's law (Bragg, 1913). XRD analysis was used to quantify the ratio of chalcopyrite and

pyrite present in the mixed mineral flotation test floated fractions and used to determine the separation efficiency of each mineral in the flotation test.

Equation 5:

$$2d(sin\theta) = \lambda_0$$

$$d = lattice\ interplanar\ spacing\ of\ the\ crystal$$

$$\theta = x - ray\ incidence\ angle\ (Bragg\ angle)$$

$$\lambda = wavelength\ of\ the\ characteristic\ x - rays$$

2.7.3.2 XRD Analysis

After the floated fraction was air dried, it was transferred onto the Mylar X-ray film window of the analysis disc. A few drops of acetone were added onto the sample and swirled until the sample was evenly distributed. The disc was then placed in the X-ray Diffractometer for analysis after the sample was air dried. Co $K\alpha_1$ [1.78892Å] radiation at 35 kV and 28 mA. The samples were analyzed from 10-90° for 10 minutes. After the data collected from the XRD analysis, Jade (McCready, 1997) was used to calculated the lattice parameters. Find it (Hellenbrandt, 2004) was used to determine the difference between the sample and library literature and then TOPAS (Celho, 2007) was used to quantify the ratio of chalcopyrite and pyrite in the sample.

2.7.3.3 Determination of Errors

A standard mixed mineral was performed to determine the errors in the XRD quantification and analysis. The standard mixed mineral has a known percentage of 49.31% chalcopyrite and 50.69% pyrite. This sample was quantitatively analyzed by XRD twice and the results were used to examine the errors.

The recovery of pyrite or chalcopyrite of the mixed minerals flotation test is calculated by equation 6. The separation efficiency is calculated by comparing the recovery of each mineral from. The impurities in chalcopyrite is 16% and 4% in pyrite. If the recovery of chalcopyrite is greater than pyrite, this indicates a positive separation efficiency.

Equation 6:

$$Recovery\ of\ Pyrite\ (100\%) = \frac{The\ percentage\ of\ pyrite\ in\ flotated\ fraction \times flotated\ fration}{The\ amount\ of\ pyrite\ used \times 0.96} \times 100$$

$$Recovery\ of\ Chalcopyrite\ (100\%) = \frac{The\ percentage\ of\ chalcopyrite\ in\ flotated\ fraction \times flotated\ fration}{The\ amount\ of\ chalcopyrite\ used\ \times 0.84} \times 100$$

3.0 Results and Discussion

3.1 Bacterial Cell Growth

As the study objective of this project was to determine the surface modification of chalcopyrite and pyrite by *A.f.*, the bacterial cell growth was monitored by bacterial counting. The change of the cell concentrations of different *A.f.* cultures over time was used to determine the growth phase of each culture.

3.1.1 *Acidithiobacillus Ferrooxidans* Grown on HH Media

The *A.f.* grown on HH media solution A and B has a growth cycle of 96 hours. The HH media solution B contains free Fe^{2+} ions and *A.f.* can use it as an energy resource. Therefore, the bacterial cell growth can be determined by both cell counts and ferrous ion concentration. As shown in Figure 5, the *A.f.* growth enters its lag phase between 0 and 22 hours after re-culture. Between 22 and 48 hours, the exponential phase of the reference culture was observed. The reference culture reaches its stationary phase between 48 and 96 hours. The *A.f.* reference culture will be re-cultured at stationary phase to keep the bacteria in the culture healthy and active.

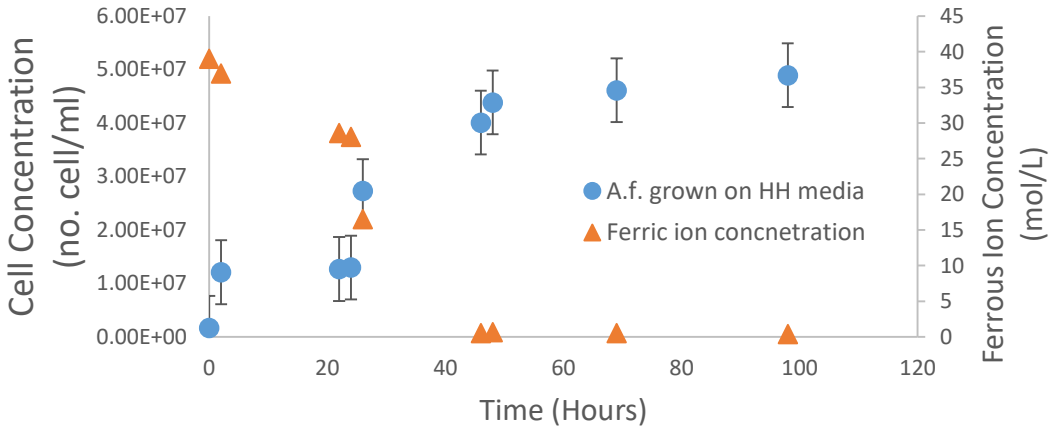

Figure 5: The bacterial growth curve of *A.f.* grown on HH media and the corresponding ferrous ion concentration.

The ferrous ion concentration will start to decrease as the culture enters lag phase. This is due to the onset of oxidation of Fe^{2+} to Fe^{3+} ions by the *A.f.* In the exponential phase of the *A.f.*, the ferrous ion concentration was dramatically reduced, indicating the ferrous ion oxidation rate is associated with the bacterial growth rate. Therefore, the growth of *A.f.* in HH media can be determined based on the change of concentration of ferrous ions in the solution over time (Belinda, 2014).

3.1.2 *Acidithiobacillus Ferrooxidans* Adjusted to Pyrite and Chalcopyrite.

Figure 6 shows the cell concentration of *A.f.* on 20g 38-75µm pyrite and chalcopyrite mineral particles. The *A.f.* will have longer growth cycle when it is grown on pyrite (28 days) than with free Fe^{2+} ions (4 days). This is because no Fe^{2+} was present in the solution and *A.f.* needs to attach to the pyrite surface in order to oxidize the $Fe^{2+}$and sulfur. The attachment between bacteria and pyrite surface requires a large amount of extracellular polymeric substances to be produced by *A.f*. Therefore, the cell replication rate needs longer time to increase. The exponential phase of *A.f.* grown on pyrite has been observed between 0 days and 12 days. Day 12 to day 28 was the stationary phase and the culture decreased after 28 days. Therefore, the culture needs to be re-cultured at day 28 to keep *A.f.* growing. Once the *A.f.* grown on pyrite culture enters its stationary phase, the cell concentration (1.4×10^8 cells/ml) was much higher than for the reference culture (5×10^7 cells/ml). This is because pyrite can provide *A.f.* with both Fe^{2+} and sulfur as its energy sources.

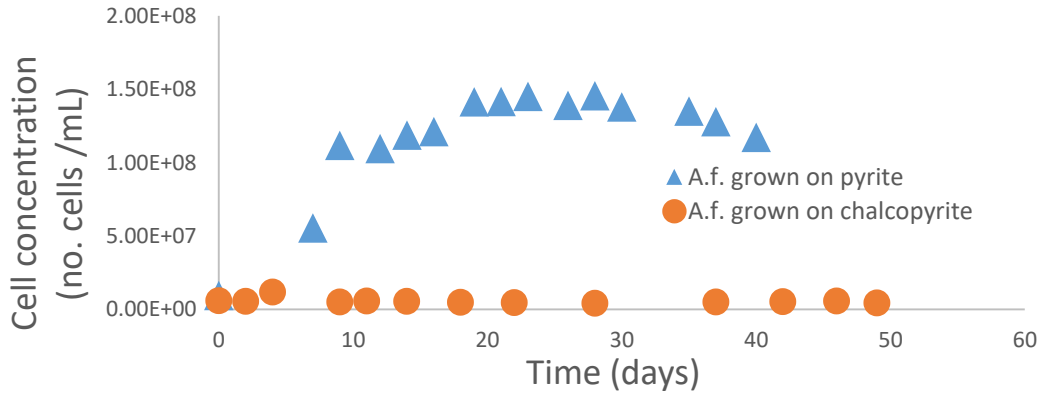

Figure 6: The cell concentration of *A.f.* grown on pyrite (blue) and chalcopyrite (red) over time.

As shown in Figure 6, the cell concentration of *A.f.* grown on chalcopyrite was significantly lower than on pyrite. It indicates *A.f.* could not be adapted and grown on chalcopyrite, probably because chalcopyrite only contains Fe^{3+} and it is slower for bacteria to be attached to the mineral surface. Another reason is that the new chalcopyrite contains about 16% of impurities some of which might be toxic to *A.f.*, e.g. Ca^{2+}. The copper toxicity of *A.f.* is the other factor may responsible for the low cell concentration (Dopson et al, 2003). Therefore, the SEM and XPS analysis of chalcopyrite was not performed.

3.1.3 *Acidithiobacillus Ferrooxidans* Adjusted to Mixed Pyrite and Chalcopyrite

A.f. were adjusted to mixed pyrite and chalcopyrite to adapt *A.f.* to chalcopyrite. Figure 7 shows, the *A.f.* growth enters its lag phase between 0 day to 27 days when *A.f.* were exposed to 10g chalcopyrite and 10g pyrite. Between day 27 and day 31, the growth of the culture was at the exponential phase. The stationary phase occurred between day 31 and day 50. The *A.f.* exposed to mixed minerals was re-cultured at its stationary phase with a lower amount of pyrite.

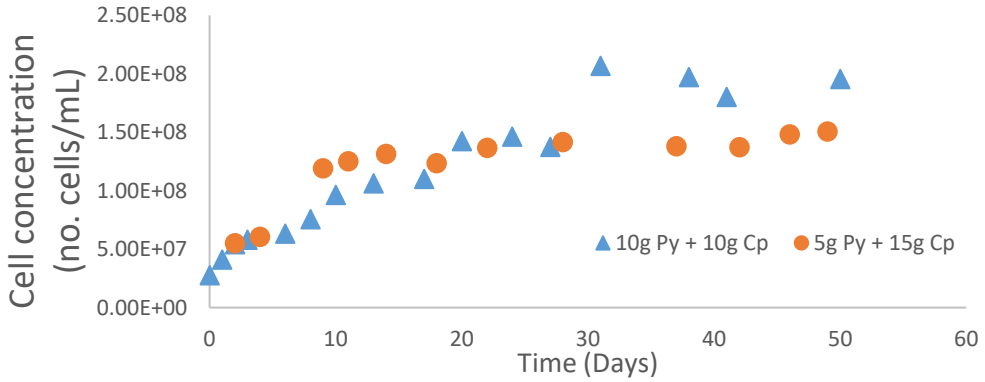

Figure 7: The growth curve of *A.f.* grown on pyrite and expose to different ratio of chalcopyrite and pyrite mixed minerals.

After the *A.f.* exposed to mixed minerals was re-cultured with a smaller amount of pyrite, the lag phase of bacterial growth started from day 0 to day 4. The exponential phase has been observed between day 4 and day 9. Between day 9 and day 49, the *A.f.* grown on mixed minerals enters its stationary phase. However, a lower cell concentration was observed during the stationary phase when the amount of pyrite decreased. Therefore, *A.f.* might not use the energy resource from chalcopyrite for its growth.

3.2 SEM analysis

SEM was used in this project to determine the time range when *A.f.* is selectively attached to the surfaces of chalcopyrite and pyrite.

3.2.1 EDX Analysis

EDX analysis was performed to distinguish chalcopyrite and pyrite in the *A.f.* expose to mixed minerals. Figure 12 presents the EDX spectra of the pyrite and chalcopyrite. The pyrite contains Fe and S signals but chalcopyrite has Cu, Fe and S signals. All SEM images from the *A.f.* exposed to mixed minerals were analysed by EDX to determine the type of mineral (Figure 8).

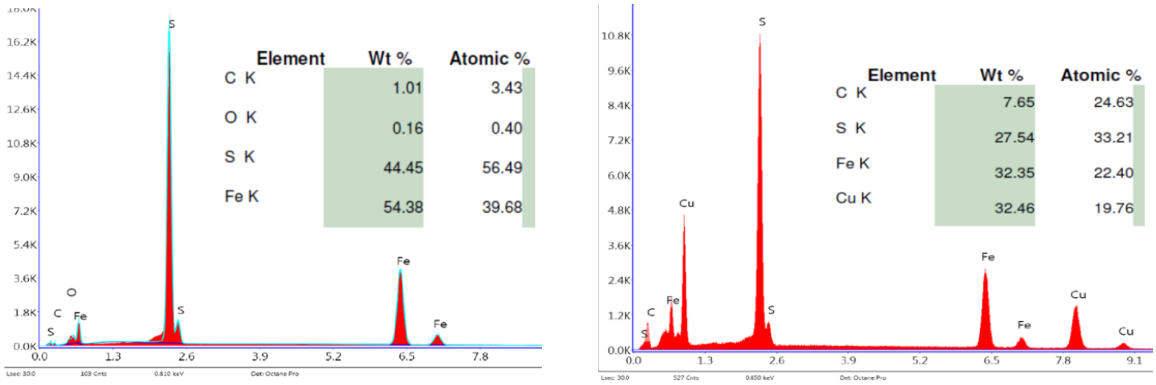

Figure 8: The chemical composition spectrum of the pyrite (left) and chalcopyrite (right) in the *A.f.* expose to mixed minerals for two hours.

The bacteria and EPS on the mineral surface were also identified by EDX analysis, e.g. Figure 9. *A.f.* is a rod-shape bacteria and it will generally create relatively higher carbon and oxygen EDX signals.

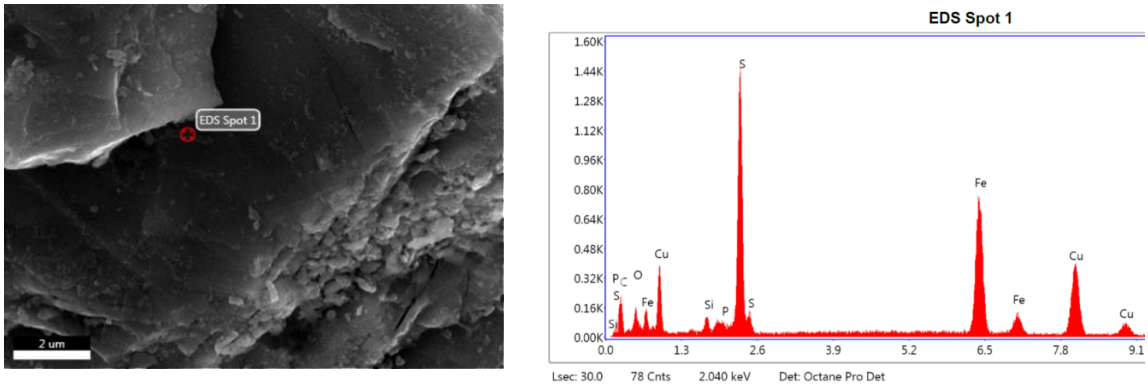

Figure 9: SEM image of *A.f.* grown on mixed mineral (left). The EDX analysis spectrum (right) of *A.f.* on the chalcopyrite surface.

3.2.2 *Acidithiobacillus ferrooxidans* Expose to Pyrite

The SEM samples of *A.f.* exposed to pyrite were taken at 2, 24, 48, 72 hours, 1 week and 2 weeks exposure time. As can be seen in Figure 10, 11 and 12, different topographies were observed on the pyrite surface at different exposure time. The *A.f.* were included in the red circle and the EPS were in the yellow circle. The amount of bacteria and EPS on the pyrite was small when pyrite was exposed to *A.f.* for 2 and 24 hours. No biofilm was observed on the pyrite surface.

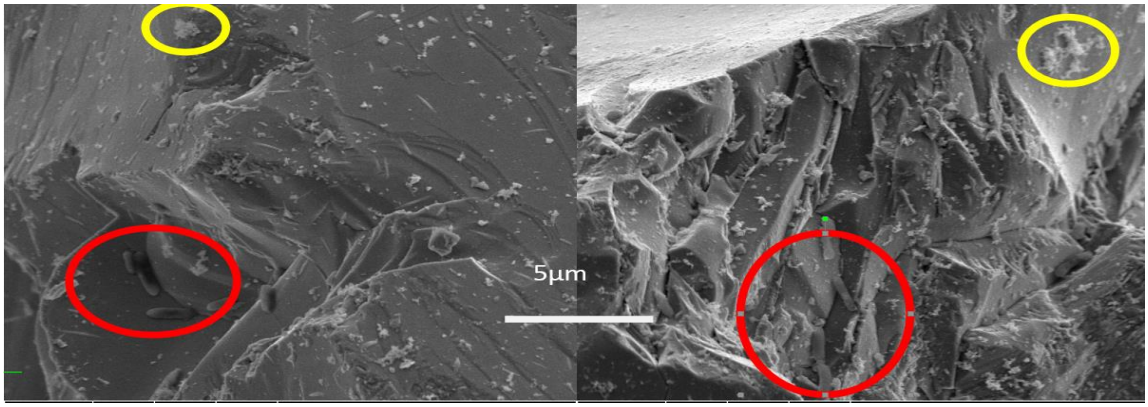

Figure 10: SEM images of pyrite mineral particles surface exposed to *A.f.* for 2 hours (left) and 24 hours (right).

As shown in Figure 11, a large amount of EPS was present on the pyrite surface exposed to *A.f.* for 48 and 72 hours. A biofilm has been indicated by the green circle on both 48 hours and 72 hours exposure sample. It shows *A.f.* starts to attach onto the pyrite surface after 48 hours exposure time and change the surface hydrophobicity of mineral particles.

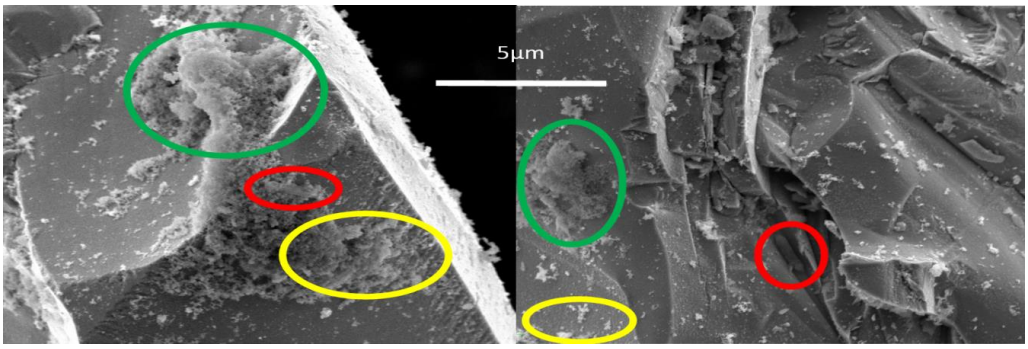

Figure 11: SEM images of pyrite mineral particles surface exposed to *A.f.* for 48 hours (left) and 72 hours (right).

A different morphology has been observed in Figure 12, no biofilm has been found on both samples of pyrite expose to *A.f.* for 1 and 2 weeks. Limited amounts of bacteria and EPS were found on the surface of pyrite. Moreover, the topography in the blue circle in both images indicates the leaching of pyrite mineral particles started in the presence of *A.f.* Therefore, the pyrite mineral particles were start to leach after exposure to *A.f.* for a week.

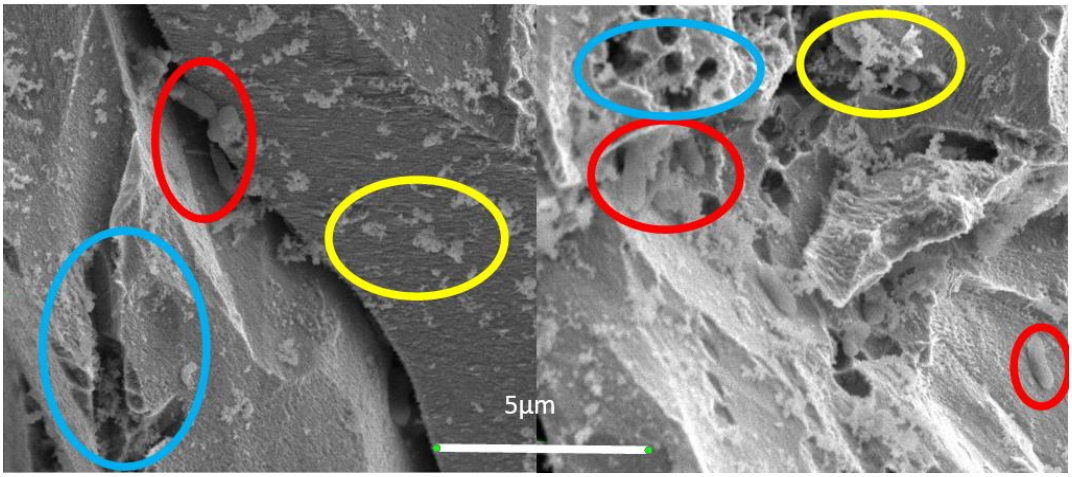

Figure 12: SEM images of pyrite mineral particles surface exposed to *A.f.* for 1 week (left) and 2 weeks (right).

3.2.2 *Acidithiobacillus ferrooxidans* Expose to Mixed Minerals

To distinguish chalcopyrite and pyrite in the mixed minerals sample, the EDX analysis spectra were obtained. After mixed pyrite and chalcopyrite were exposed to *A.f.* for 2 hours, the topography of both mineral surfaces were very similar. A few bacteria (red circle) and EPS (yellow circle) were observed on both chalcopyrite and pyrite surface (Figure 13). Based on the SEM sample preparation processes, the mineral samples were washed by a different concentration of ethanol several times. Therefore, any free bacteria in the solution will be washed off. Therefore, the images (Figure 13) indicate there is no selective attachment of *A.f.* on chalcopyrite and pyrite after 2 hours exposure time. As shown in Figure 18, more bacteria (red circle) were present on both chalcopyrite and pyrite surfaces when the minerals were exposed to *A.f.* for 24 hours. No significant amount of EPS was present on the surfaces of both minerals.

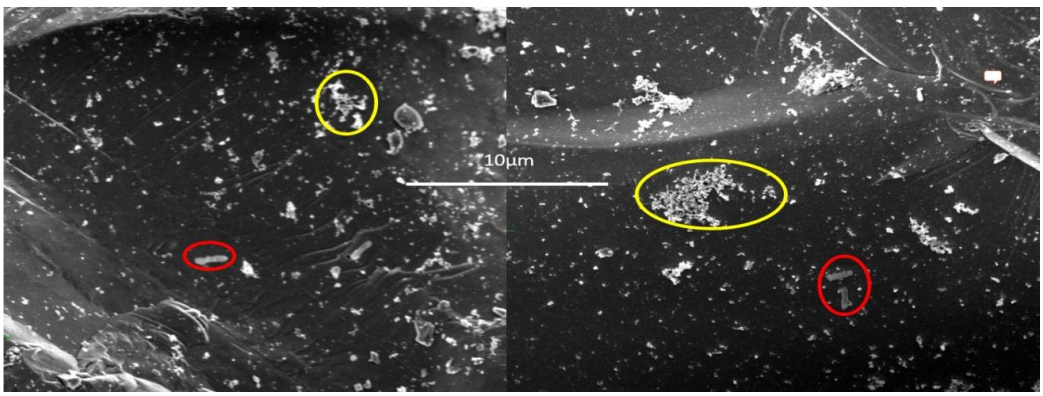

Figure 13: SEM images of chalcopyrite (left) and pyrite (right) surface exposed to *A.f.* for 2 hours.

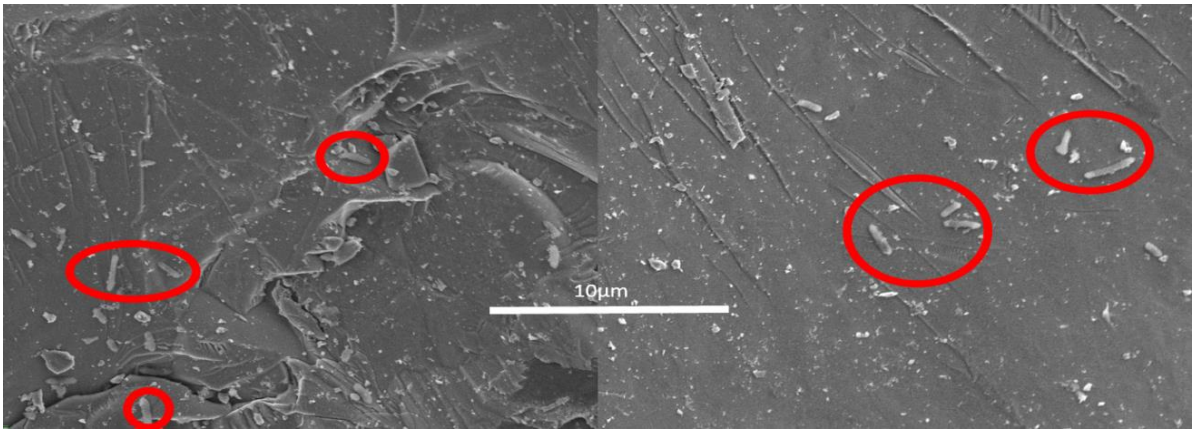

Figure 14: SEM images of chalcopyrite (left) and pyrite (right) surface exposed to *A.f.* for 24 hours.

When mixed minerals were exposed to *A.f.* for 48 hours, a significant amount of EPS (yellow circle) were performed on chalcopyrite and pyrite surface (Figure 15). The amount of bacteria on both mineral surface almost has no change as compared to the 24 hours sample. No biofilm has been identified on the surfaces of both minerals and no leaching effects were observed.

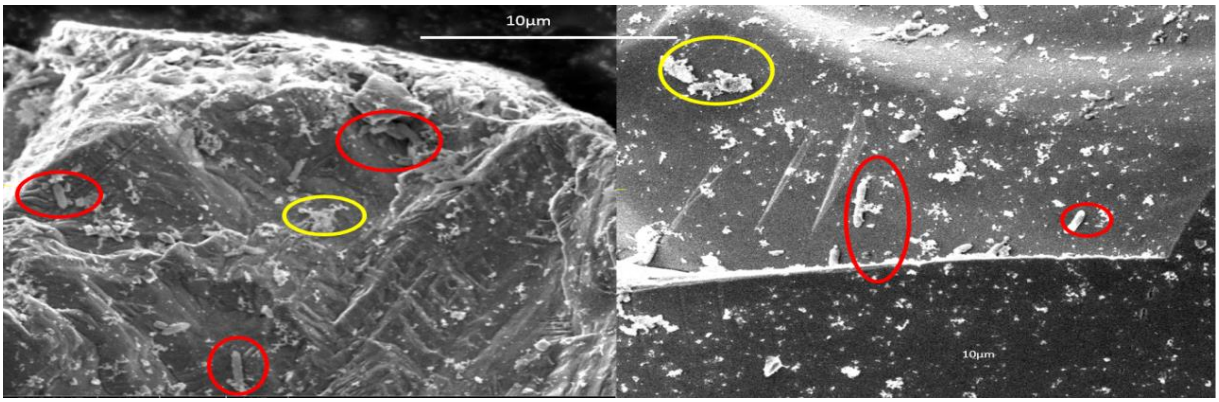

Figure 15: SEM images of chalcopyrite (left) and pyrite (right) surface exposed to *A.f.* for 48 hours.

A significant amount of bacteria were shown on the pyrite surface after the mixed minerals were exposed to *A.f.* for 72 hours (Figure 16). After exposure for 1 week, a large group of EPS was present on the chalcopyrite surface but no biofilm formed. A limited scale of leaching effects (Blue circle) was also observed on both mineral surfaces. Therefore, both chalcopyrite and pyrite mineral particles in a mixed sample were start to leach upon expose to *A.f.* for 72 hours.

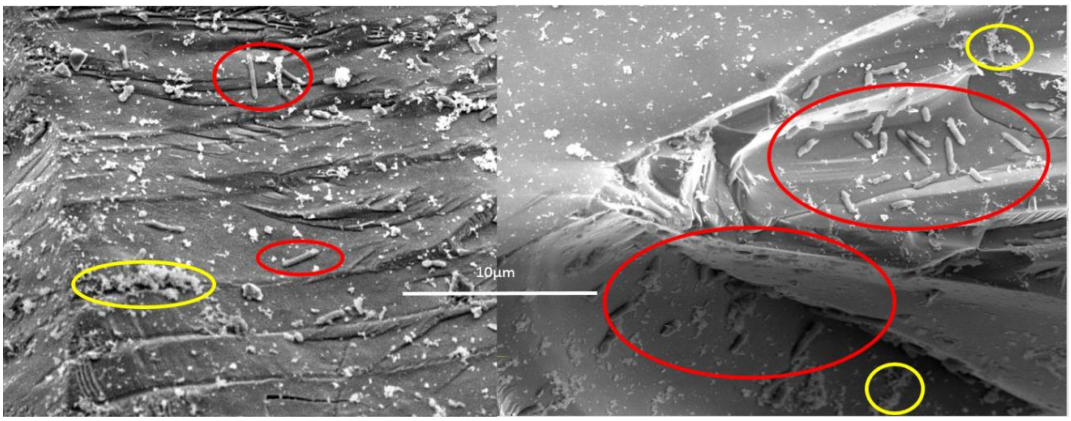

Figure 16: SEM images of chalcopyrite (left) and pyrite (right) surface exposed to *A.f.* for 72 hours.

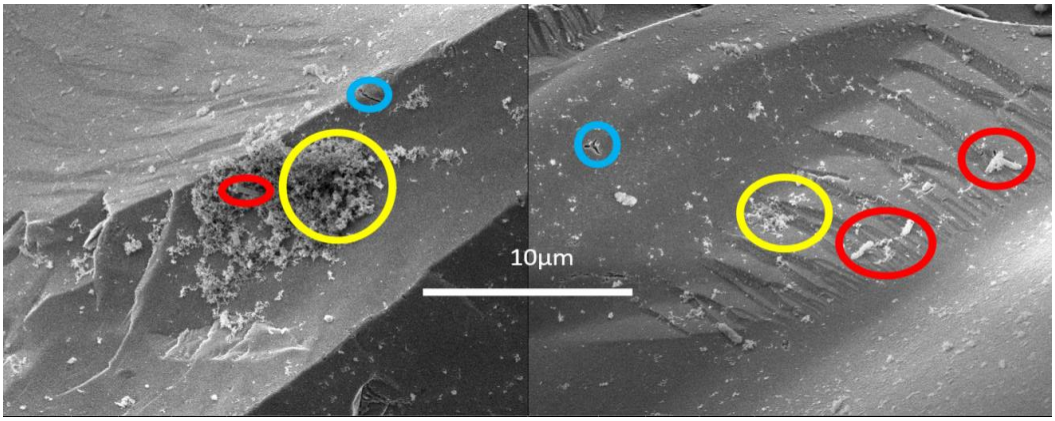

Figure 17: SEM images of chalcopyrite (left) and pyrite (right) surface exposed to *A.f.* for a week.

As shown in Figure 18, a significant leaching effect by *At. ferrooxidans* was found on pyrite surface after exposure for over 2 weeks. More bacteria existed on chalcopyrite surface than pyrite.

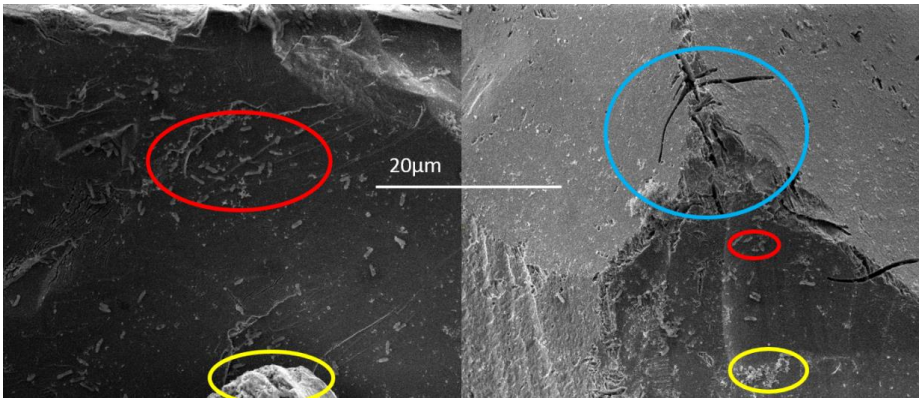

Figure 18: SEM images of chalcopyrite (left) and pyrite (right) surface exposed to *A.f.* for two weeks.

The SEM images from *A.f.* grown on mixed mineral samples indicate that there is no selective attachment of *A.f.* to the chalcopyrite and pyrite after 2 hours exposure time. The bacteria, EPS, chalcopyrite and pyrite were identified using EDX analysis.

3.3 X-ray Photoelectron Spectroscopy (XPS) Analysis

3.3.1 Surface Element concentration

Figure 19 is an example of survey spectrum of pyrite. The atomic concentrations obtained from the survey scans of all samples are presented in Table 3. The blank sample was made by exposing 20g pyrite to HH media solution A at pH 1.8 for 24 hours, 48 hours, 72 hours and 1 week. Carbon is the most abundant element on most samples and contributes to 30-50% of the surface composition, except pyrite expose to HH media for 24 hours. This is due to the loss of Fe on the surface and sulfur-rich layer was exposed and conduct the unreasonable high sulfur signal. Adventitious carbon was the major source contributing to the relatively high carbon signal. In the sample exposed to *A.f.*, bacteria and extracellular polymeric substances on the pyrite surface also contributed to the increase of carbon signal. A relatively high signal of oxygen has been observed in most samples. Oxides, hydroxides, the attached and absorbed water were the major sources contributing to the oxygen signal (Harmer et al., 2006). Due to the presence of C_{18}-C_{20} fatty acid and glucuronic acid, a small amount of oxygen signals on the bacteria-exposed sample are contributed by EPS (Bagdigian & Myerson, 1986). A decrease in iron concentration on the pyrite surface was observed in most samples. The relative Cu concentration was contributed by the impurities in pyrite (Chapter 2.1). An increase of S/Fe ratio has been observed in the bacteria-exposed sample but the ratio consistently decreased as the exposure time increased, indicating *A.f.* preferentially oxidizes the iron in the pyrite first and leaves a sulfur-rich layer on the pyrite surface. The decrease in the S/Fe ratio as the exposure time increased indicates the sulfur atom on the pyrite surface was oxidized by bacteria.

Table 3: The surface composition (atomic concentration %) of pyrite exposed to HH media or *A.f.* at 30°C (*hv* = 1487 eV).

Sample	C 1s (284.8eV)	S 2p (162.4eV)	O 1s (531.0eV)	Fe 3p (53eV)	Cu 2p (932.7eV)
Unreacted Pyrite	41.7%	29.4%	21.4%	6.7%	0.9%
Blank 24 hours	32.1%	39.1%	19.6%	7.4%	1.8%
A.f. 24 hours	45.4%	22.6%	27.8%	4.0%	0.2%
Blank 48 hours	47.7%	22.2%	25.0%	4.8%	0.4%
A.f. 48 hours	39.2%	24.4%	31.7%	4.2%	0.6%
Blank 72 hours	44.9%	22.0%	28.3%	4.4%	0.4%
A.f. 72 hours	47.1%	17.8%	30.9%	3.2%	1.0%
Blank 1 week	39.1%	27.7%	27.8%	5.3%	0.2%
A.f. 1 week	44.2%	12.2%	38.9%	4.0%	0.8%

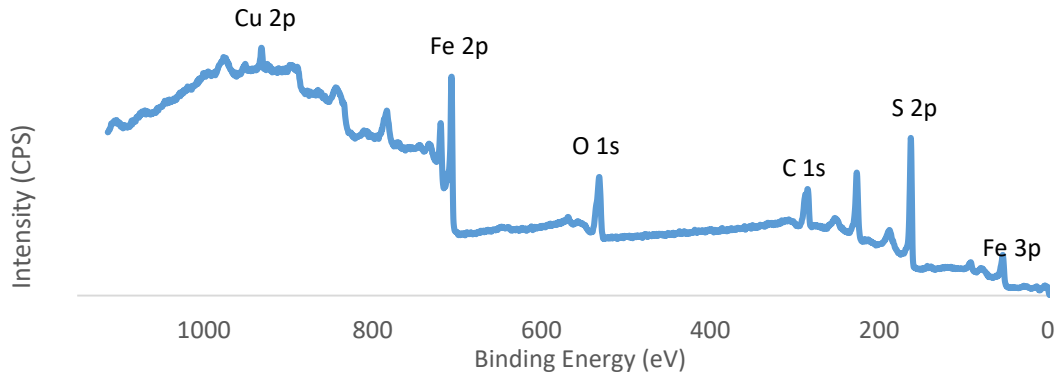

Figure 19: The survey spectrum of an unreacted pyrite (*hv* = 1487 eV).

3.3.2 Sulfur 2p Spectra

High resolution sulfur 2p spectra of pyrite exposed to *A.f.* at 30°C were obtained at a photon energy of 1487 eV and presented in Figure 20 and 21. The most intense S $2p_{3/2}$ peak at 162.4 eV is due to the bulk disulfide. The disulfide species are located at 161.6 eV. Polysulfide (S_n^{2-}) and elemental sulfur (S^0) have a binding energy in the range of 163-163.9 eV (Buckley and Woods, 1984; Harmer et al., 2006; 2004). The absence of S peaks around 168.0 eV suggests that there is no sulfate on the unreacted pyrite surface (Figure 20). Therefore, the unreacted pyrite was only slightly oxidized prior to exposure to HH media and *A.f.*

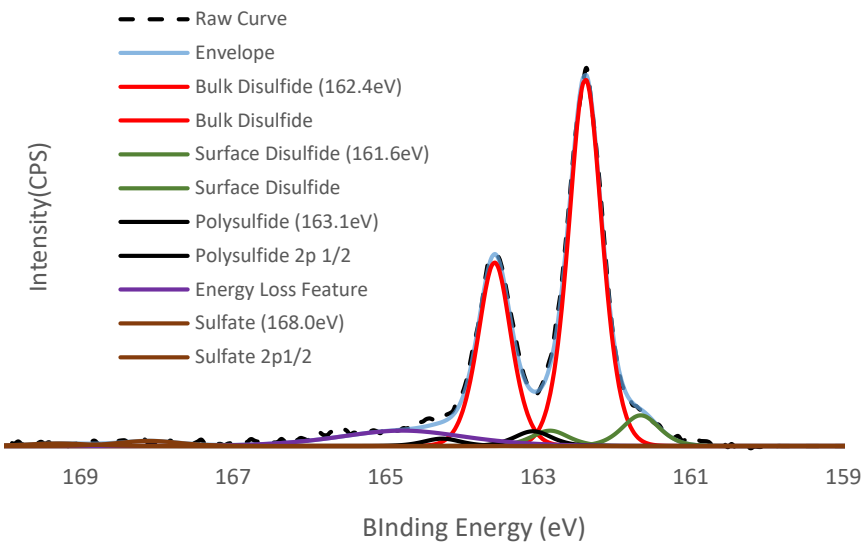

Figure 20: The fitted sulfur 2p spectra of unreacted pyrite.

According to Figure 20 and 21, the amount of bulk disulfide and surface disulfide on pyrite exposed to *A.f.* did not change within 72 hours. Moreover, there is no indication of the formation of polysulfide formed by *A.f.* on the surface. No remarkable increase of the sulfate peak at 168 eV in Figure 21 A, B and C was observed. Therefore, *A.f.* is not able to modify the pyrite surface sulfur layer within 72 hours exposure time. After pyrite was exposed to *A.f.* for a week, the sulfur layer in pyrite surface were significantly changed. As shown in Figure 21D, the bulk disulfide S $2p_{1/2}$ peak was dramatically reduced as compared to unreacted pyrite (Figure 20). No change was observed from the surface disulfide peak. However, both polysulfide and sulfate peaks significantly increased. The result indicates the sulfur layer of pyrite surface was oxidized by *A.f.* and a large amount of polysulfide and sulfate were formed after 168 hours exposure. A comparison of the sulfur 2p spectra of pyrite at -168°C (Figure 21) and 20°C (Figure 34 in appendix), a significant amount of elemental sulfur has been observed at about 164.3 eV until pyrite expose to *A.f.* for 1 week.

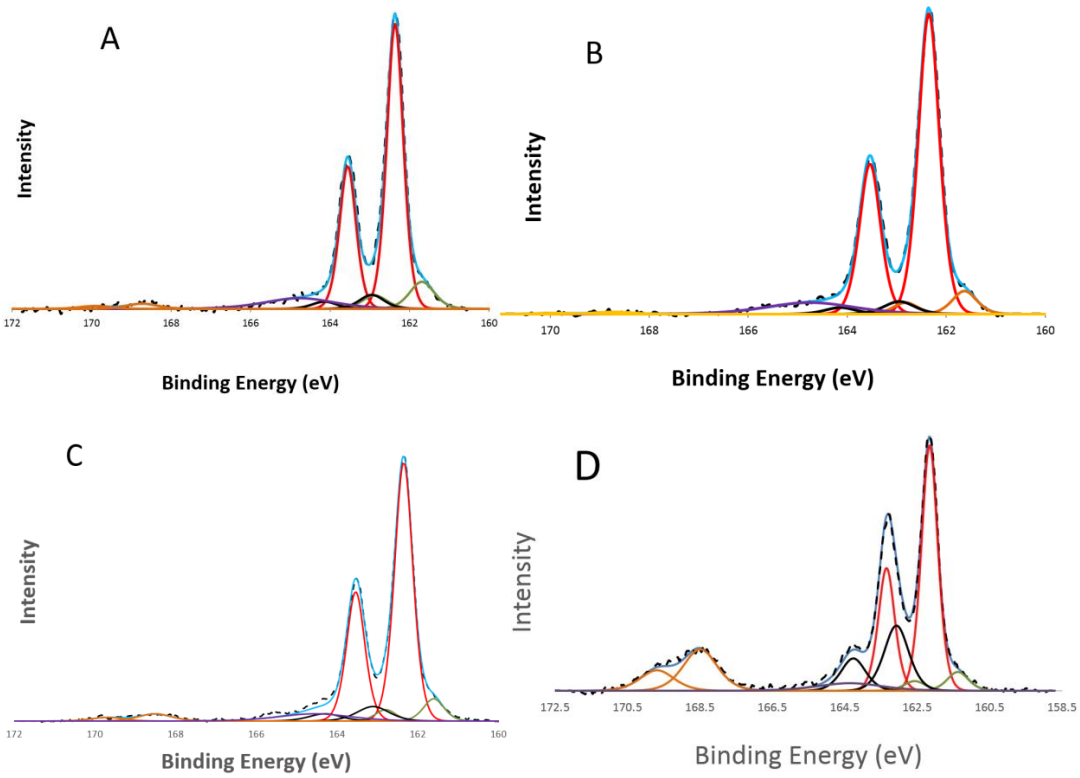

Figure 21: The surface modification of pyrite surface sulfur layer exposed to *A.f.* at 30°C. (A, exposed for 24 hours; B, exposed for 48 hours; C, exposed for 72 hours; exposed for 168 hours)

3.3.3 Iron 2p spectra

The Fe 2p spectra of unreacted pyrite is displayed in Figure 22. The peak at 707.1 eV represents Fe (II) in the bulk pyrite. The Fe (II)-S and Fe (III)-S features on the pyrite surface are located at 708.3 eV and 709.1 eV respectively. The oxidized Fe features are generally located at 710.8-713.8 eV (Gupta and Sen, 1975; Schaufuβ and Nesbitt, 1998, Harmer and Nesbitt, 2004). Figure 23 shows, those Fe species on the pyrite surface were not affected by HH media solution A at pH 1.8 within 1 week exposure time. There is no significant variation in the Fe 2p spectra of pyrite exposed to *A.f.* for different times (Figure 23). Therefore, *A.f.* is not able to significantly oxidize Fe on the pyrite surface within 1 week.

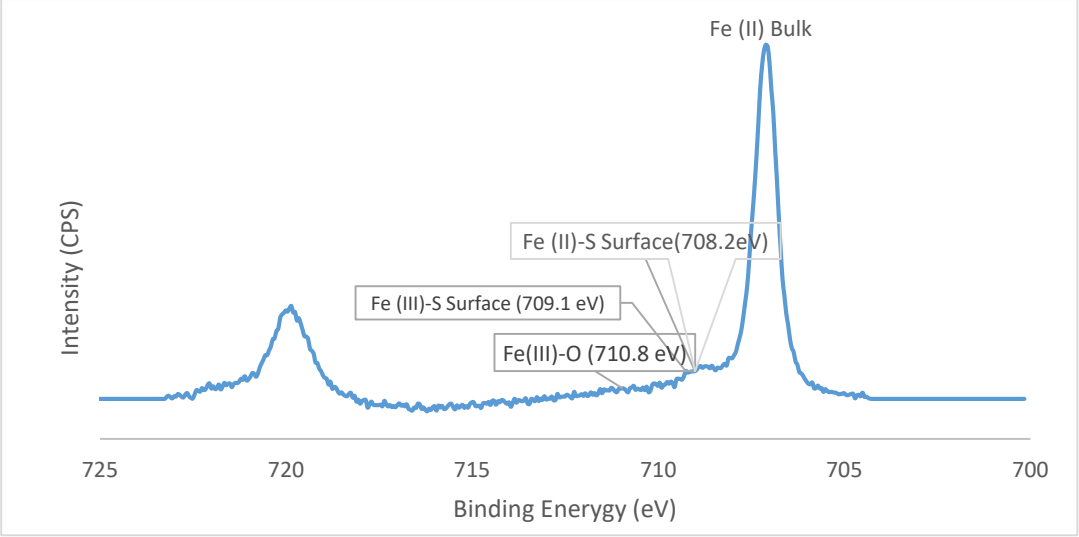

Figure 22: The Fe 2p spectra of unreacted pyrite.

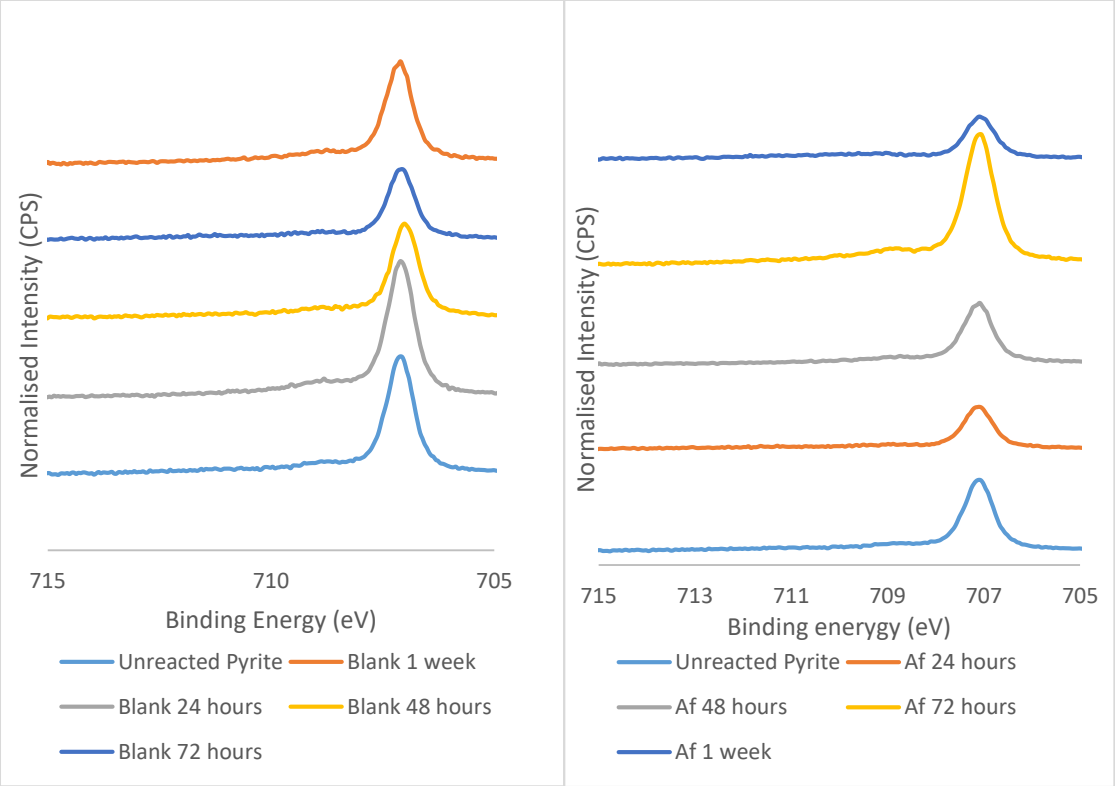

Figure 23: The Fe 2p spectra of pyrite expose to HH media with (right) and without *A.f.* (left) at pH 1.8 and 30°C from 24 hours to 168 hours.

3.3.4 Carbon 1s Spectra

Most carbon signals on the pyrite surface are contributed by C-H peak from polysaccharides and bacteria. As shown in Figure 24, the observed C-H signal at 284.8 eV is contributed by adventitious carbon and polysaccharides from *A.f.* EPS. EPS also contains proteins, C_{18}-C_{20} fatty acids and glucuronic acids (Bagdigian & Myerson, 1986). Moreover, *A.f.* itself is also composed of some organic compounds. Therefore, proteins in EPS and bacteria are the major

sources of C-N (286.0 eV) and N-C=O (290 eV) peaks (Ray and Shard, 2011). C-O signal at 286.3 eV and C=O signal at 287.6 eV were also observed due to adventitious carbon, e.g. CO, CO_2 in the air (Miller and Biesinger, 2001). The observation of O-C=O peak (289.0 eV) indicates the presence of fatty acid and polysaccharides.

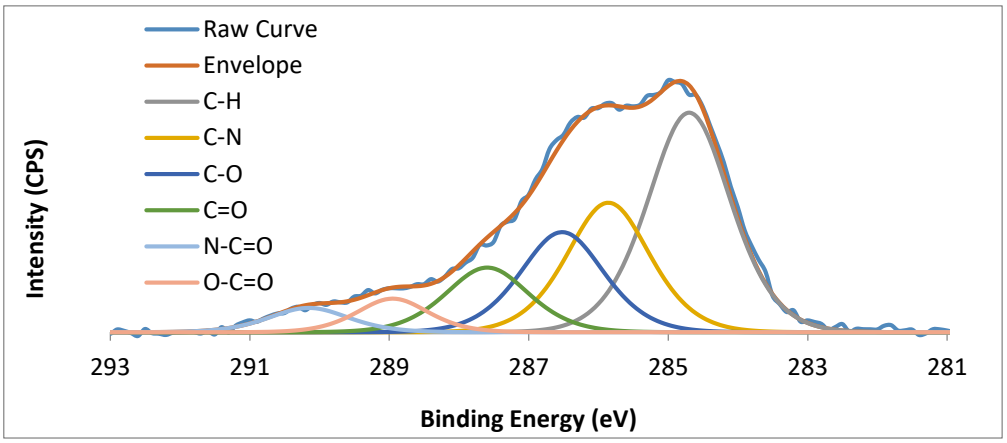

Figure 24: The fitted carbon 1s spectra of pyrite expose to *A.f.* at pH 1.8 and 30°C for 1 week.

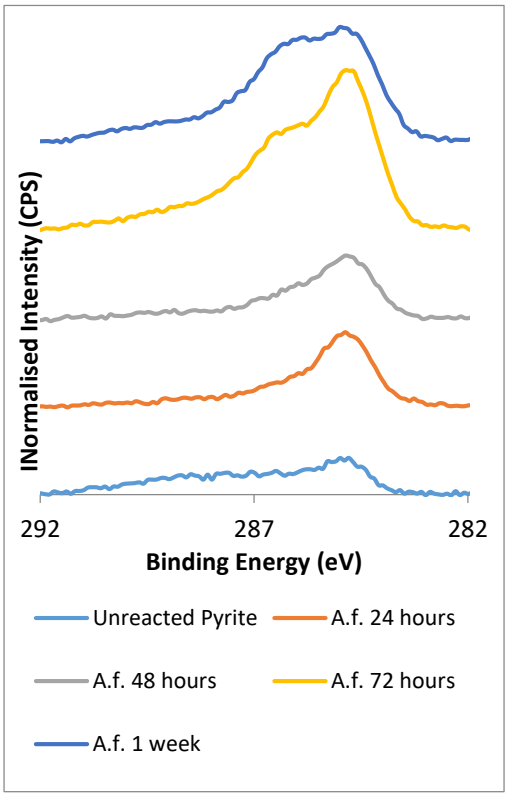

Figure 25: The carbon 1s spectra of pyrite expose to A.f. at pH 1.8 and 30°C from 24 hours to 168 hours.

As Figure 25 illustrated, the C-H, C-N and C-O peaks slightly increased with time pyrite during exposure to *A.f.* in the first 48 hours. According to the results from SEM images of *A.f.* exposed to pyrite for 24 and 48 hours, more bacteria were observed than for the 2 hours sample, resulting in the increased carbon signal. Moreover, a biofilm was observed on the pyrite surface when exposed to *A.f.* for 48 hours. The O-C=O and N-C=O signals both slightly increased after 48 hours exposure due to the formation of protein and fatty acid in the biofilm and EPS. The carbon 1s spectra of pyrite expose to *A.f.* for 72 hours and 1 week (Figure 25) indicate a large amount of EPS were formed on pyrite surface. This is due to a significant increase of C-H, N-C=O and O-C=O peak have been observed.

3.4 Mixed Mineral Flotation Test

All flotation experiments were conducted at 0.4 L/min for 5 mins as it can produce the optimal air bubble size for flotation test with 38-75µm mineral particles (Belinda, 2014).

3.4.1 Baseline Recovery

The baseline flotation tests were conducted using 1g 50/50 synthetic mixed minerals in NaOH at pH 9 and HH media solution A at pH 1.8 at time zero. 0.09g (with recovery efficiency of 3%) of minerals were recovered from NaOH baseline flotation test. It consisted of 57.8% pyrite and 42.2% chalcopyrite. The recovery efficiency of pyrite and chalcopyrite are both 3.1%. From the baseline experiment in HH media, 0.07g of mixed minerals were recovered and the overall recovery efficiency is 1.5%. The recovered fraction contained 59.5% pyrite and 40.5% chalcopyrite. The recovery efficiency of pyrite and chalcopyrite are 1.8% and 1.2% respectively.

3.4.2 Flotation Test under Different Conditions

Table 4: The average mass and yield of mixed minerals recovered from flotation test under different conditions.

	Exposure time								
	24 hours			**48 hours**			**72 hours**		
Exposure Conditions	**Mass (g)**	**Yield (%)**	**St dev**	**Mass (g)**	**Yield (%)**	**St dev**	**Mass (g)**	**Yield (%)**	**St dev**
HH Media	0.4880	48.51	2.23	0.5334	53.92	2.46	0.5069	49.97	5.52
	0.5308	57.16	17.94	0.5317	52.97	0.90	0.4854	45.67	16.41
NaOH pH 9	0.1824	13.23	1.45	0.0643	0.42	0.03	0.0742	1.91	0.3
	0.3582	35.74	4.78	0.3082	31.51	0.20	0.5514	59.06	5.88
***A.f.* on HH Media**	0.1731	12.35	5.81	0.1168	5.99	2.42	0.1473	9.64	1.92
	0.0684	0.82	0.01	0.1707	11.96	0.55	0.0801	2.11	1.14
***A.f.* on Pyrite**	0.0638	0.59	0.29	0.0647	0.41	0.08	0.0624	0.17	0.13
	0.1091	5.42	1.18	0.0698	0.95	0.12	0.0635	0.30	0.10
***A.f.* on Mixed**	0.0664	0.81	0.32	0.0782	2.06	0.01	0.0615	0.16	0.02
Collector less				**With PIPX**					

Table 4 suggests the addition of collector (PIPX) has a significant increase on the recovery of flotation test in NaOH but not in HH media. When the mixed sample was exposed to *A.f.*, the recovery efficiency was dramatically depressed even with the addition of collector. The result also indicates *A.f.* is able to suppress the floatability improvement by collector.

3.4.3. Mineral Composition of Recovered Mixed Samples

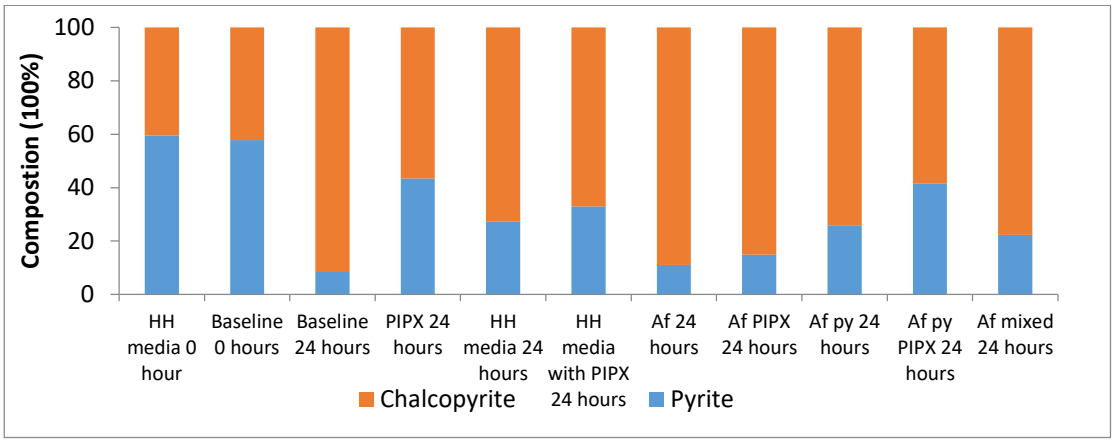

Figure 26: The average pyrite and chalcopyrite composition of recovered mixed samples after 24 hours with and without the presence of PIPX.

As Figure 26 illustrated, the composition of chalcopyrite in all of recovered mixed samples increased after 24 hours exposure in comparison to baseline results. After 24 hours exposure in NaOH and *A.f.* in HH media, the chalcopyrite composition is dramatically increased. The pyrite content increased under all conditions with the addition of collector (PIPX). The result indicates *A.f.* preferentially attached to pyrite within 24 hours exposure, resulting in the reduction of recovery of pyrite. Moreover, the Cu^{2+} formed by the oxidation of chalcopyrite might be adsorb on pyrite surface (negatively charged), enabling attachment of PIPX. Therefore, the addition of collector (PIPX) is able to improve the recovery of pyrite.

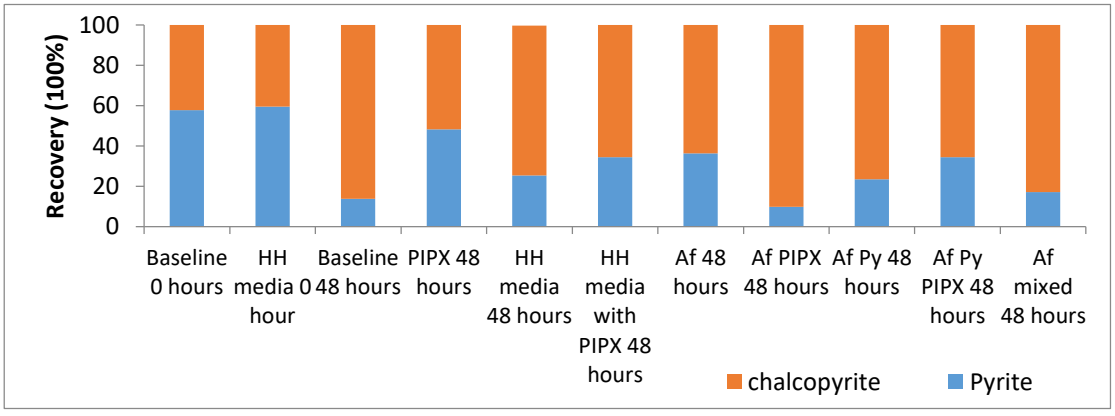

Figure 27: The average pyrite and chalcopyrite composition of recovered mixed samples after 48 hours with and without the presence of PIPX.

As Figure 27 shown, the chalcopyrite composition in recovered mixed samples increased after 48 hours exposure to all conditions compare to the NaOH and HH media baseline flotation test. A greater chalcopyrite composition was obtained with the addition of collector.

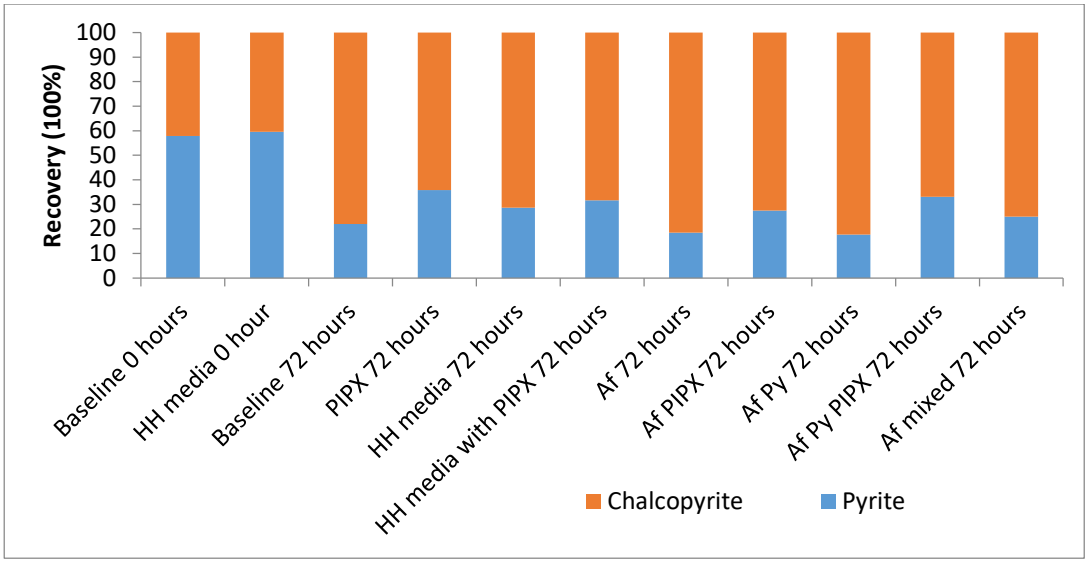

Figure 28: The average pyrite and chalcopyrite composition of recovered mixed samples after 72 hours with and without the presence of PIPX.

All recovered mixed samples from 72 hours exposures were collected and the compositions of chalcopyrite and pyrite in the floated fraction are shown in Figure 28. In comparison to the baseline of NaOH and HH media, an increase in chalcopyrite content was observed under all conditions. According to the results of flotation test with collector, no change in mineral composition was observed. Therefore, the mineral composition is very consistent when mixed samples are exposed to any conditions with collector for 72 hours.

3.4.4 Flotation Efficiency

The objective of this project was to achieve higher recovery of chalcopyrite than pyrite in mixed mineral flotation test. The flotation efficiencies were determined by comparing the recovery of chalcopyrite and pyrite. When the greater recovery of chalcopyrite than pyrite observed, it indicates a positive separation efficiency. Conversely, negative separation efficiency indicates a higher pyrite recovery than chalcopyrite. As Figure 29 shown, the recovery of pyrite is lower than chalcopyrite under all condition after exposure for 24 hours. The best separation efficiency has been observed in HH media with and without PIPX.

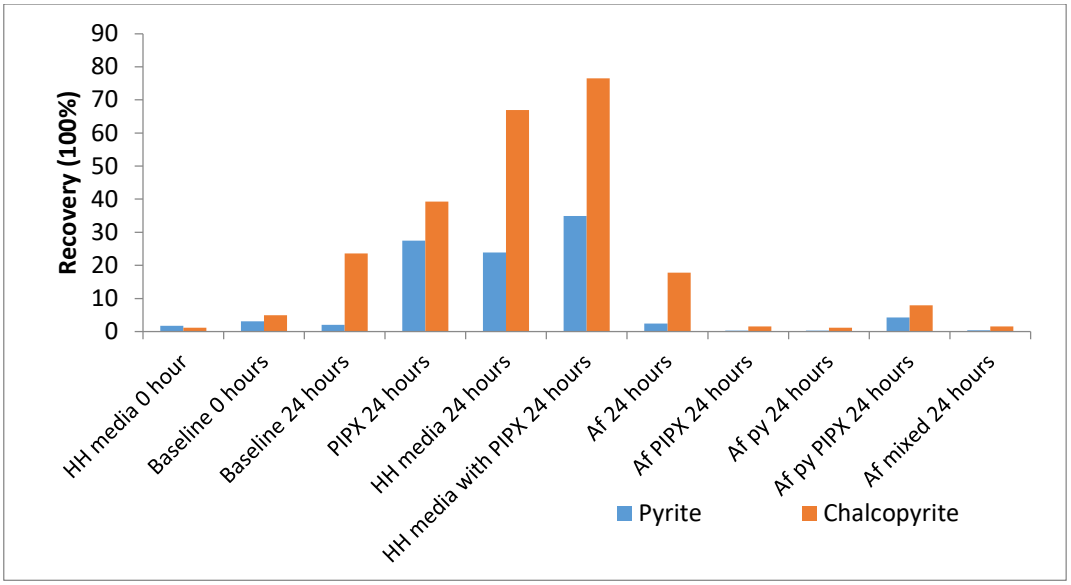

Figure 29: The recovery (%) of chalcopyrite and pyrite from mixed mineral flotation test expose to different conditions for 24 hours.

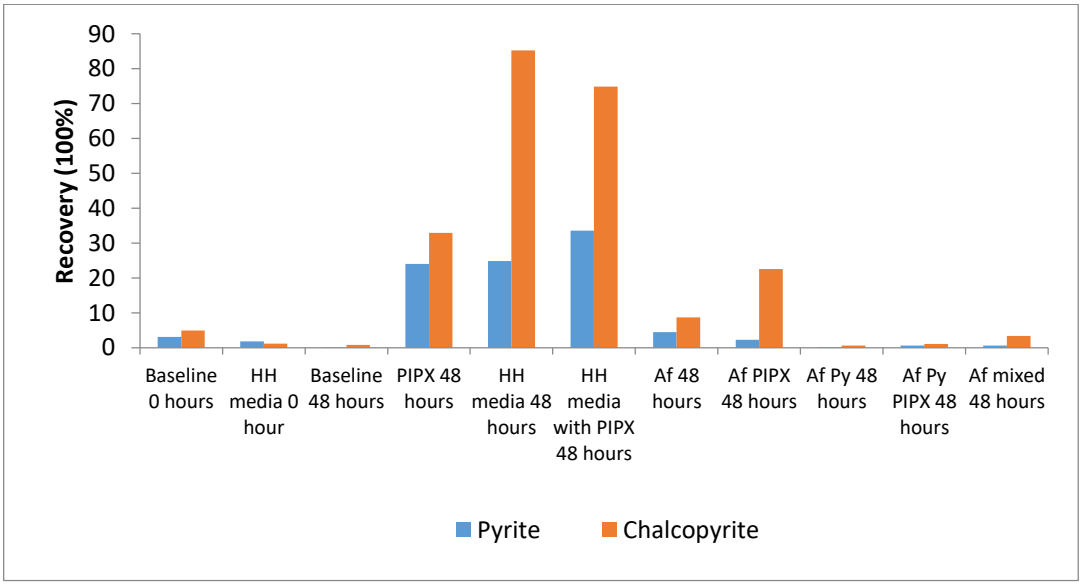

Figure 30: The recovery (%) of chalcopyrite and pyrite from mixed mineral flotation test expose to different conditions for 48 hours.

After mixed minerals were expose to different conditions for 48 hours, all flotation results indicated positive separation efficiency (Figure 30). The best separation efficiency has been observed when mixed sample exposed to HH media. After mixed minerals were exposed to *A.f.* grown on HH media for 48 hours, relatively better recovery efficiency was observed with the addition of PIPX. This indicates *A.f.* grown on HH media might be selectively attached to pyrite surface, as compare to chalcopyrite surface, and inhibits the adsorption of PIPX after 48 hours exposure.

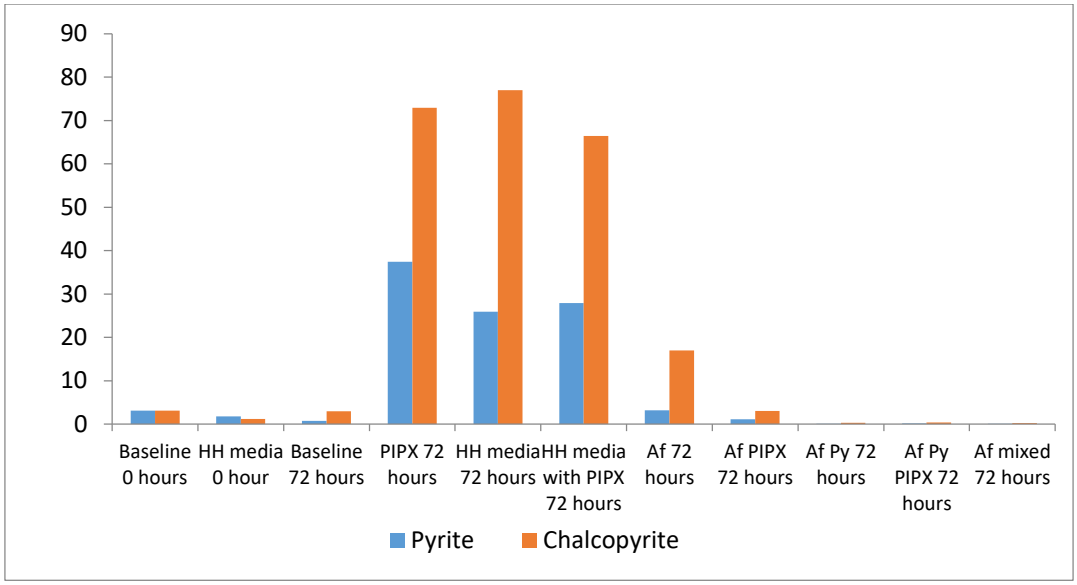

Figure 31: The recovery (%) of chalcopyrite and pyrite from mixed mineral flotation test expose to different conditions for 72 hours

After mixed minerals were exposed to different conditions for 72 hours, almost no floated fractions were collected from *A.f.* grown on pyrite and *A.f.* grown on mixed minerals sample (Figure 31). All other conditions resulting in positive separation efficiency. The best separation efficiency result at 72 hours exposure was collected from the HH media. *A.f.* grown on HH media is able to significantly depress the recovery of pyrite in mixed minerals flotation test.

4.0 Conclusion

In conclusion, *Acidithiobacillus ferrooxidans* could not be adapted and grown on the chalcopyrite mineral particles. The impurities of chalcopyrite, copper toxicity and shorter adapting time are the main causes. *A.f.* were successfully adjusted and grown on pyrite as the culture was continually re-cultured for 4 years and contains less impurities. The growth curve of *A.f.* grown on HH media and iron titration results indicate *A.f.* can grow more rapidly with free Fe^{2+} ions in the solution than with minerals.

SEM images indicate a large amount of EPS was produced by *A.f.* after it was grown on pyrite for 48 hours. After 72 hours exposure, a biofilm formed on the pyrite surface and leaching effects on pyrite were observed after 1 week. The SEM images of *A.f.* exposed to mixed mineral have not shown any selective attachment by *A.f.* on pyrite and chalcopyrite.

The XPS survey scan results indicate *A.f.* obtained energy from the oxidation of sulfur and iron to support its growth. Sulfur-rich layer was produced between 24 hours to 48 hours exposure (relative high S/Fe ratio). Sulfur 2p spectra suggest that *A.f.* was not able to oxidize the sulfur and made significant change on sulfur-layer until 1 week exposure. No significant change on Fe 2p spectra made by *A.f.* has been observed, indicating no Fe (II) or Fe (III) ions were dissolved into solution at pH 1.8 within one week exposure. Carbon 1s spectra suggested *A.f.* produced a large amount of EPS after 48 hours, supported by SEM images results.

The mixed mineral bio-flotation tests show that *A.f.* grown on HH media is able to selectively depress the recovery of pyrite at 24 and 72 hours exposure and produce a very positive separation efficiency. All pre-conditioning flotation tests resulted in positive separation efficiency. The best separation efficiency results were consistently carried out from the HH media condition with and without PIPX at 24, 48 and 72 hours exposure time.

5.0 Future Work

Future work includes the adapting of *A.f.* on chalcopyrite and take more sufficient results of the surface modification of chalcopyrite by XPS and SEM and determine the selective attachment of *A.f.* on chalcopyrite and pyrite.

A further research could be conducted to investigate the roles of EPS in surface modification and its application in bio-flotation. Further chemical analysis of EPS produced by *A.f.* grown on different minerals might be interested.

Appendix

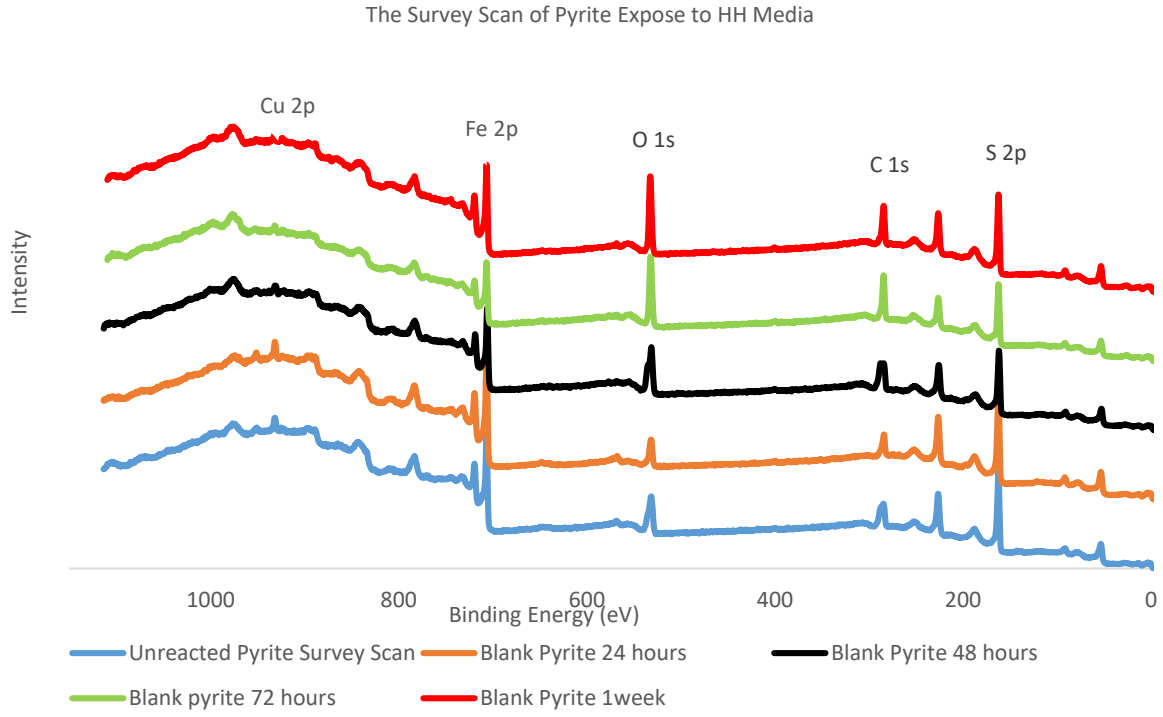

Figure 32: The Survey Scan of Pyrite Expose to HH Media at pH 1.8 from 24 hours to 168 hours.

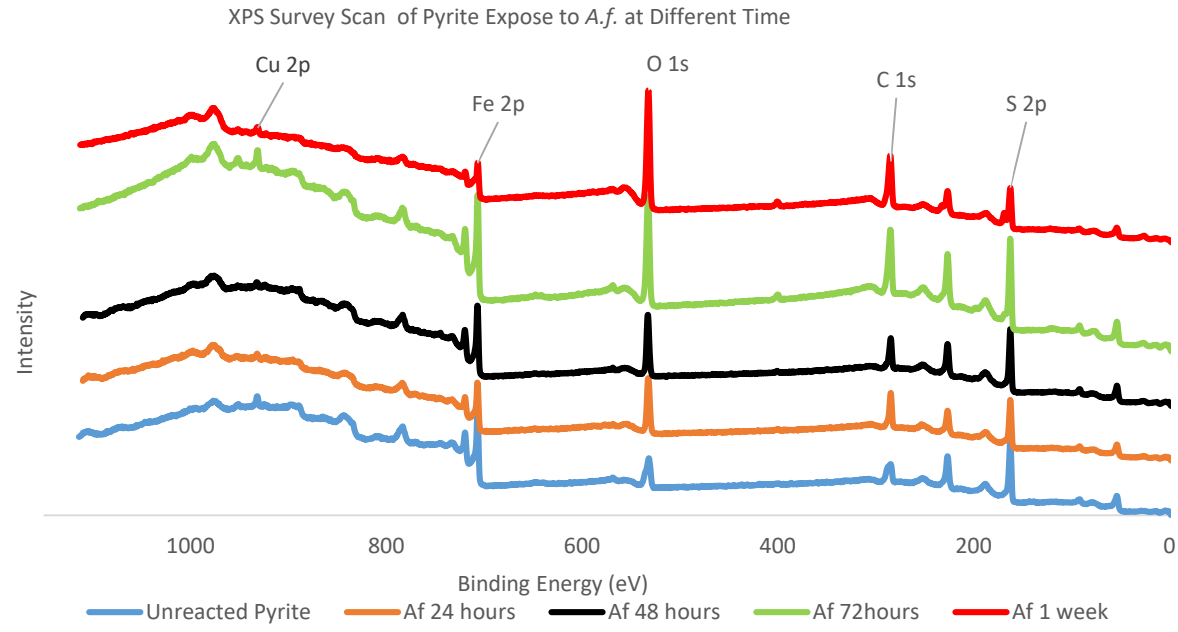

Figure 33: The Survey Scan of Pyrite Expose to *A.f.* at pH 1.8 from 24 hours to 168 hours.

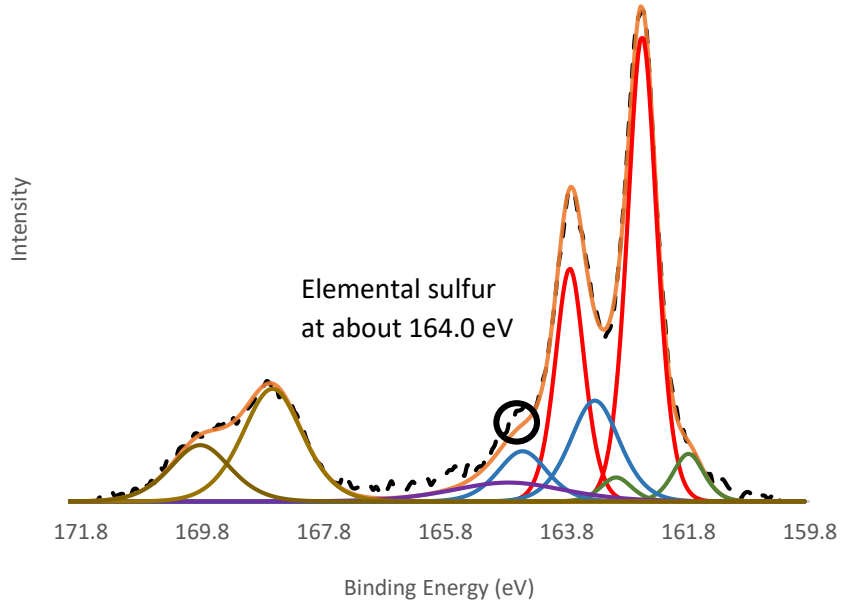

Figure 34: The Sulfur 2p spectra of pyrite expose to *A.f.* at pH 1.8 for 1 week. Sample taken at 20°C.

Reference

Acres, R.G., Harmer S.L., Beattie, D.B., 2010. *Synchrotron XPS, NEXAFS, and ToF-SIMS studies of solution exposed chalcopyrite and heterogeneous chalcopyrite with pyrite.* Minerals Engineering Vol23 p.g.928-936.

Australian Bureau of Statistics. 2003. *Mining and the environment.* Year Book Australia. Viewed on 6th Nov 2017. Available from: http://www.abs.gov.au/ausstats/abs@.nsf/90a12181d877a6a6ca2568b5007b861c/ce28d7fbe5faa308ca256cae0015da32!OpenDocument

Besser, J and et al. 2009. *Ecological impacts of lead mining on Ozark streams: toxicity of sediment and pore water.* Ecotoxicology and Environmental Safety. Vol 72 (2) p.g.516-526

Bleeze, B 2014. *Separation of chalcopyrite and pyrite though bio-flotation.* Honours thesis. Flinders University. Adelaide. Australia.

Bragg, W.H.*;* Bragg, W.L. *1913*. *The Reflexion of X-rays by Crystals.* Proc R. Soc. Lond. A. **88** (605): 428–38.

Coelho, A.2007. *Bruker AXS,* Karlsruhe, Germany.

Dopson, M and et al. 2003. *Growth in sulfidic mineral environments: metal resistance mechanisms in acidophilic micro-organisms.* Microbiology, Vol149 p.g.1959-1970

Dhau, J.S., Singh, A. Sooch, B. S., Brandão, P. and Félix, V. 2014. *Journal of Organometallic Chemistry* Vol *766* p.g.57-66.

Fairley, n. 2009. *CasaXPS Manual*, Version 2.3.16Dev52, Casa Software Ltd. http://www.casaxps.com.

Fankhauser, D.B. 2004. *Bacterial Growth Curve.* University of Cincinnati Clermont College.

Finch, J.A. and Dobby, G.S. 1990. *Column Flotation,* Pergamon Press, Oxford.

Freund, M. and Carol, B. 1964. *Journal of reproduction and fertility.* Vol *8*, p.g.149-155.

Goldstein, J. 2003. *Scanning Electron Microscopy and X-Ray Microanalysis.* Springer.

Goldstein, G. I. et al. 1981. *Scanning electron microscopy and x-ray microanalysis.* New York: Plenum Press.

Gupta, R.P. and Sen, S.K. 1975. Phys. Rev. B 12 (1) 15–19.

Harmer, S.L. and Nesbitt, H.W. 2004. *Stabilization of pyrite (FeS_2), marcasite (FeS_2), arsenopyrite (FeAsS) and Loellingite ($FeAs_2$) surfaces by polymerization and auto-redox reactions*. Surface Science. Vol564 p.g.34-52.

Harmer, S.L., Thomas, J.E., Fornasiero, D., Gerson, A.R., 2006. *The evolution of surface layers formed during chalcopyrite leaching.* Geochimica et Cosmochimica Acta 70, p.g.4392-4402.

Hazeu W, Batenburg-van der Vegte WH, and et al. 1988. *The production and utilization of intermediary elemental sulfur during the oxidation of reduced sulfur compounds by Thiobacillus ferrooxidans.* Arch Microbiol. Vol.150: p.g.574-579.

Hellenbrandt, M. 2004. *Crystallography Reviews*, Vol*10* p.g.17-22

Hosseini TR, Kolahdoozan M and et al. 2005. *Bioflotation of Sarcheshmeh copper ore using Thiobacillus ferrooxidans bacteria*. Miner Eng. Vol 18 p.g.371-374.

Jenkins, R. and Snyder, R. L. 2012. *Introduction to X-ray Powder Diffractometry.* Vol138 p.g.48-95.

Kolahdoozan M and et al. 2004. *Bioflotation of low grade Sarcheshmeh Copper sulfide.* Trans Indian Inst Met. Vol 57 p.g.485-490.

McMullan, D. 2006. *Scanning Electron Microscopy 1928-1965*. Scanning. Vol17 p.g. 175-185.

McCready, D.E, Balmer, M.L. and Keefer, K.D.1997. *Powder Diffraction.* Vol*12* p.g.40-46.
Miller, D.J., Biesinger, M.C. and et al. 2002. *Interactions of CO_2 and CO at fractional atmosphere pressure with iron and iron oxide surfaces: one possible mechanism for surface contamination?.* Surf. Interface Anal. Vol33 p.g.299-305

Moulder, J.F., Stickle, W.F., Sobol, P.E. and Bomben, K.D. 1995. *Handbook of X-ray Photoelectron Spectroscopy.* Physical Electronics, Inc. The United States of America. p.g. 9-14

Misra M, Chen S. 1995. *The effect of growth medium of Thiobacillus ferrooxidans on pyrite and galena flotation*. In: Holmes DS, Smith RW, eds. Minerals Bioprocessing II, The Minerals, Metals and Materials Society, Pennsylvania, p.g.313-322.

Mussel, W. N., Murad, E., Fabris, and et al. 2007. *Characterization of a chalcopyrite from 26 Brazil by Mo¨ssbauer spectroscopy and other physicochemical techniques.* Physics and 27 Chemistry of Minerals. Vol. 34, p.g.383-387.

Pecina-Treviño ET, Ramos-Escobedo GT, Gallegos-Acevedo PM, López-Saucedo FJ, Orrantia-Borunda E. 2012. *Bio-flotation of sulfide minerals with Acidithiobacillus ferrooxidans in relation to copper activation and surface oxidation.* Canadian Journal of Microbiology; Vol 58, p.g.1073–83.

Ray, S. and Shard, A.G. 2011. *Quantitative Analysis of Adsorbed Proteins by X-ray Photoelectron Spectroscopy*. Anal. Chem. Vol83 p.g.8659-8666.

Rohwerder, T., Sand, W., 2003. The sulfate sulfur of persulfides is the actual substrate of the sulfur-oxidizing enzymes from *Acidithiobacillus* and *Acidiphilium* spp. Microbiology. Vol 149, p.g.1699-1709.

Schaufuβ, A.G. and Nesbitt, H.W. 1998. *Incipient oxidation of fractured pyrite surfaces in air.* Journal of Electron Spectroscopy and Related Phenomena. Vol96 p.g.69-82.

Schippers A, Sand W. 1999. *Bacterial leaching of metal sulfide proceeds by two indirect mechanisms via thiosulfate or via polysulfides and sulfur. Appl Environ Microbiol*. Vol 65 p.g.319-321.

Schippers A, Jozsa P-G, Sand W. 1996. *Sulfur chemistry in bacterial leaching of pyrite.* Appl Environ Microbiol. Vol 62 p.g.3424-3431.

Vaughan, D.J. and Craig, J.R. 1978. *Mineral Chemistry of Metal Sulfides*. Cambridge University Press Cambridge.

Wills, B.A. 2011. *Froth-flotation*. Wills' Mineral Processing Technology: an introduction to the practical aspects of ore treatment and mineral recovery, Vol 12, p.g.267-282.

Xu, Y.; Lay, J. P.; Korte, F. (1988). *"Fate and effects of xanthates in laboratory freshwater systems".* Bulletin of Environmental Contamination and Toxicology. Vol **41** (5): p.g.683–689.